Front. Earth Sci. 2024, 18(2): 422–445
https://doi.org/10.1007/s11707-024-1114-1

RESEARCH ARTICLE

Quantitative assessment of the supply, demand and flows of ecosystem services in the Yangtze River Basin, China

Dongjie GUAN (✉), Xiaofeng FAN, Lilei ZHOU, Kangwen ZHU

School of Smart City Institute, Chongqing Jiaotong University, Chongqing 400074, China

Abstract Ecosystem service flow is essential for transporting, transforming, and maintaining ecosystem services and connecting supply and demand. This study attempted to quantitatively assess the supply and demand flows of ecosystem services in the Yangtze River Basin in 2000, 2010, and 2020; assess the evolution of the spatial patterns of ecosystem service flow at the provincial, watershed and urban agglomeration scales; and design a zoning standard for ecosystem service flow. The results showed as follows. 1) Between 2000 and 2020, the Yangtze River had a progressive drop in its freshwater supply, water conservation service and carbon sequestration service flows. The decline rates for these services were measured at 10.90%, 11.11%, and 5.17%, respectively. The climate regulation service flow exhibited a pattern of initial fall followed by a subsequent increase, characterized by a decline rate of 35.53%. 2) The lowest was the ecosystem service flow in the lower reaches of the Yangtze River and the Yangtze River Delta urban agglomeration. Freshwater supply service flow and water conservation service flow were the highest in the upper reaches of the Yangtze River and the Chengdu-Chongqing urban agglomeration. Carbon sequestration service flow and climate regulation service flow were the highest in the middle reaches of the Yangtze River Basin and the urban agglomeration in the middle reaches of the Yangtze River. 3) From 2000 to 2020, the change ratios of the area proportion of the confluence, flow, and outflow areas in the Yangtze River Basin were 1.06, 3.17, and 0.86, respectively. The results of this research could offer decision support for regulating ecosystem services in the Yangtze River Basin, promoting sustainable regional development and achieving rational use of the basin resources.

Keywords Yangtze River Basin, ecosystem services, supply and demand, service flow, quantitative assessment, spatial matching

Received July 4, 2023; accepted December 13, 2023

E-mail: guandongjie_2000@163.com

1 Introduction

Ecosystem services (ES) are the natural surroundings and impacts of ecosystem formation and maintenance of human activities and comprise various direct or indirect benefits that humans derive from ecosystem functions (Fisher et al., 2009). The supply of ES indicates that the ecosystem provides services and products for humans, and the demand entails the consumption and usage of the goods and services produced by the ecosystem (Tao et al., 2022). Ecosystem service flow describes the dynamic process of a few transitive and liquid ES throughout a specific time period in various spatial contexts (Lin et al., 2021). Quantitative characterization of ecosystem service flow can effectively illustrate the criticality of ES to human wellbeing (Schirpke et al., 2019). The assessment of the supply and demand flows of ES can help to measure the contribution of nature to humans and illuminate the link between the supply and demand, thus promoting regional planning and policy formulation, and facilitating regional sustainable development (Wang et al., 2022b).

The evaluation methods of the ecosystem service supply mainly include the ecological model method (Du et al., 2023; Xue et al., 2023), value method (Liu et al., 2023a; Zhang et al., 2023), and participation method (Wang et al., 2022c; Tindale et al., 2023). Most of them quantitatively evaluate the ecosystem service supply by coupling and integrating other indicators or statistical methods with the help of mature and suitable ecological models such as InVEST (Zhang and Li, 2022; Hu et al., 2023), SWAT (Zhang et al., 2022b; Tan et al., 2023b), SolVES (Duan and Xu, 2022; Zhang et al., 2022a) and RUSLE (Geng et al., 2022; Yan and Li, 2023). Liu et al. (2023c) evaluated the impact of land use change on the

water balance in a typical loess hilly sub-basin in China. Zhu (2022) used the SolVES model to quantitatively measure the cultural ecosystem services in the region from the perspectives of social attributions and spatial heterogeneity. In addition to the more intuitive ecological model method of the spatial effect, there are widely used methods such as the expert evaluation method, equivalent factor method and service function price method with fewer data requirements. Müller et al. (2020) constructed an expert matrix method to evaluate the ecosystem service potential of terrestrial, coastal and oceanic ecosystem types in northern Germany. Abdelrhman et al. (2022) assessed the economic value of ES offered by the Drangi forest in Sudan using the contingent valuation approach. Jiang et al. (2022) quantified various eco-compensation criteria and ecosystem service values in the Yangtze River Economic Belt using incremental ES and opportunity cost methodologies. In summary, the ecological model method still suffers technical problems, such as model algorithm optimization and parameter correction, and the data requirements for the considered study area are relatively high. Due to diverse scales and sophisticated calculating procedures, the evaluation outcomes of the value method are readily affected. The participation method can truly reflect the respondent' awareness of ES and is suitable for research at different scales, but the notable subjectivity affects the reliability and accuracy of quantitative assessment.

The evaluation of the ecosystem service demand mostly adopts statistical methods (Shaad et al., 2022; Xia et al., 2022), and empirical methods (Brooks et al., 2020; Liu et al., 2022b) but lacks a more intuitive and balanced spatial expression. Vergarechea et al. (2023) assessed the timber and biomass needs of Norwegian forests to achieve mitigation targets. Hochmalová et al. (2022) mapped the social needs of forest ecosystems in the study areas of the Czech and China. The demand for ES in an Andalusian olive orchard in southern Spain was spatially analyzed by Granado-Díaz et al. (2020) using the replacement index approach. Based on various indicators, Sauter et al. (2019) evaluated the demand for flood protection, adjacent recreation, and biodiversity in the Austrian Folalberg Mountains. Stürck et al. (2014) utilized the economic loss in the basin and the upper basin region to represent the demand for flood control services. Scholars focus on supply-side quantification when quantifying ES and address the assessment of demand for ES, mainly by combining supply and demand for ES to assess ecosystem service flows. In summary, in terms of estimating demand for ES, there is a lack of more accurate models and more balanced spatial expression methods (Xiang et al., 2022; Xu and Peng, 2022; Yin et al., 2023). Setting scenarios and employing geographically distributed models to gauge ecosystem service demands will become popular issues in ecosystem service research as academics pay greater attention to the quantification of ES (Lin et al., 2022; Yang et al., 2022b; Zhao et al., 2022).

The main method of quantitatively evaluating ecosystem service flow entails the use of a spatially distributed model to quantitatively analyze and map the supply and demand, transmission route and transmission process of ES (Wu et al., 2022; Xu and Zhang, 2022). The most typical methods are service path attribution networks (SPANs) (Qin et al., 2019) and Bayesian belief networks (BBNs) (Dang et al., 2020). SPANs employ an artificial intelligence-based model research approach to analyze the flow of ES from supply to benefit regions (Schuwirth et al., 2019). However, the model contains many parameters during operation that must be localized based on differences within the research area. To study the supply-demand flows of various supply, regulatory, and cultural service types in the Spanish Doana National Park and its environs, Palomo et al. (2013) employed the expert evaluation approach. Serna-Chavez et al. (2014) identified the spatial location of various types of ecosystem service supply areas, service radiation ranges and demand areas and introduced the supply-demand ratio index to explore ecosystem service flow. Leveraging Bayesian networks, Feurer et al. (2021) modeled and mapped nine ES for local stakeholders in Daning Dayi, Myanmar. Due to the diversity and complexity of ES, it is impossible to use models to simulate the actual transmission process and the pathways of ES. In the future, constructing an ecosystem service flow model should fully use existing multisource data to reveal the dynamic process of ecosystem service flow.

The Yangtze River Basin (YRB) not only comprises a complex ecosystem but also comprises a significant ecological security barrier region in China (Fang et al., 2021). Over the past 20 years, due to the continuous growth in population pressure, high-intensity development of water and soil resources, and the reduction in the stability of ecosystem circulation under climate change and other natural and human factors, environmental pollution in the YRB has intensified, and ecological damage, frequent natural disasters and resource shortages in some areas remain prominent, resulting in imbalances between economic and social development and resources and the environmental carrying capacity, which has become a major bottleneck restricting the sustainable development of the YRB. Understanding the variations, interactions, and influencing factors of ES in watersheds is essential for water ecosystem management and regulation. Quantitative evaluation of the supply, demand and flow of ES can serve a scientific foundation for the formulation of ecological preservation initiatives and environmental management strategies.

Regional disparities in the supply, demand and flow of ES are prevalent due to the diverse environmental and economic conditions (Yu et al., 2021; Jia et al., 2023; Jiang et al., 2023). Regional planners employ zoning as a

spatial tool to streamline information for subsequent analysis and management when confronted with numerous spatial entities, including administrative units and features (Wang et al., 2022b; Gao et al., 2023). Wu et al. (2023) constructed a spatial flow model of ES and proposed a management strategy for optimizing the spatial pattern of urban agglomerations in the Pearl River Delta. The establishment of regional ecological zoning through the evaluation of ecosystem service supply, demand, and flow in spatial and temporal dimensions is beneficial for the development of more scientifically and logically grounded ecological protection policies (Shi et al., 2020; Wu et al., 2023; Yan et al., 2023). By reviewing the above research progress, we believe that existing studies have made positive progress in assessing the supply and demand of ES, the evolution of the spatial and temporal distribution of ES, and the flow of ES. There are still some issues, though. The first is the absence of a more precise method to measure the supply, demand and flow of ES (Wang et al., 2022b; Xiang et al., 2022; Xu and Peng, 2022); the second is the absence of research on the evolution of supply, demand, and flow and the spatial matching relationship at the watershed scale (Huang et al., 2022; Zhou et al., 2022; Guan et al., 2023); and the third is the lack of research on the zoning design for regulating the mismatch between supply and demand of ES from the perspective of supply, demand and flow relations (Assis et al., 2023; Lyu and Wu, 2023; Yuan et al., 2023).

Against this background, this paper explores the following research questions. 1) How to quantify the supply, demand and flow of ES in the YRB? 2) What are the spatio-temporal dynamic characteristics and trends of supply, demand and flow of ES in the YRB? 3) How to put forward regulatory ways to optimize the ecosystem service flow in the YRB?

To answer these questions, first, the InVEST model was used to quantitatively evaluate the supply, demand and flow of ES in the YRB from 2000 to 2020, and the temporal and spatial variation of supply, demand and flow of ES in the YRB in the past 20 years was analyzed. Secondly, spatial autocorrelation analysis and other methods were used to identify the hotspots of supply and demand for watershed ES. From the provincial, watershed and urban agglomeration scales, the spatial heterogeneity and mismatch characteristics of the supply and demand relationship were clarified by comparing the actual flow of ES to human beings and the supply capacity of ES. Finally, the spatial pattern evolution trend of ecosystem service flow in the YRB was used to divide and design the flow of ES. A regulatory path was also suggested for improving the flow of ES.

2 Materials and methods

2.1 Study area

The YRB refers to the vast area flowing through the mainstream and tributaries of the Yangtze River (Fig. 1), located at 24°30′–35°45′N, 90°33′–122°25′E. southwest China, central China, and east China are the three principal regions covered. The basin covers an area of around 1.8 million km^2 or 18.8% of China's total land area (Yang et al., 2022a). With abundant hydropower resources, mineral resources and forest resources, it is a significant ecological treasure house in China. The typical urban agglomerations of the Yangtze River Delta urban agglomeration (YRDUA), the middle reaches of Yangtze River urban agglomerations (MRYRUA), and the Chengdu-Chongqing urban agglomeration (CCUA) have been formed in the basin. According to the 2021 China Statistical Yearbook, the population of the basin reached 513 million in 2020, making up 36.34% of the country's overall population. The entire output value of regional production is 58.69 trillion Yuan, or 57.97% of the overall output value in China. It is one of the core areas of the Chinese economic growth. Ecosystem protection in the YRB is effective, but the improvement in the water environment quality varies, and the protection and

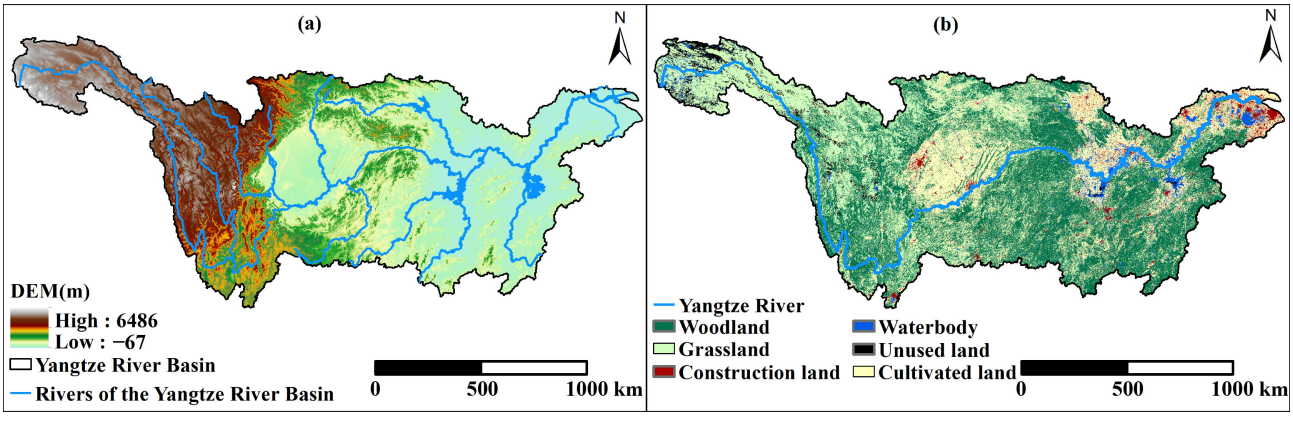

Fig. 1 Study area.

restoration of the ecosystem must be strengthened (Zheng et al., 2020). In 2018, the water quality standards in critical water functionality zones in the YRB reached only 79.9%. In 2020, the proportion of sections with excellent water quality (grades I–III) in the YRB was 88.7% (Song et al., 2023). According to the Announcement of Soil and Water Conservation in the Yangtze River Basin (2020), soil and water loss in the YRB was 337000 km^2, accounting for 18.81% of the basin area in 2020. Compared to that in 2018, the water and soil area of the YRB decreased by 9700 km^2 in 2020, a decrease of 2.80%.

2.2 Data sources

The main data sets required in this study included socioeconomic data, land use data, natural environment data, as summarized in Table 1. This study uses population density and GDP data to calculate the demand for freshwater services and carbon emissions from 2000 to 2020. Since the population density data and GDP data in 2020 cannot be obtained, the population density data and GDP data in 2019 will replace the data in 2020 in combination with the statistical bulletin of the People's Republic of China on national economic and social development in 2020 and the China Statistical Yearbook 2021. 2000–2020 population density and GDP data from Resource and Environment Science and Data Center.

2.3 Construction of the ecosystem service supply assessment model

2.3.1 Freshwater supply assessment model

This paper regards the freshwater supply (*FS*) as ecosystem services value provided by the YRB to the outside world (Zhang et al., 2021). Based on a large amount of measured spatial data for the study area, the freshwater supply service supply (*FSS*) was evaluated on the ArcGIS10.4 software platform with the InVEST model (Zhou et al., 2021; Li et al., 2022). The *FSS* can be calculated as follows:

$$WY_x = \left(1 - \frac{AET_x}{P_x}\right) \times P_x, \tag{1}$$

where WY_x is the water yield of the raster cell (mm), AET_x is the average annual evapotranspiration of the raster cell x (mm), and P_x is the average annual precipitation of the raster cell x (mm). AET_x/P_x represents the ratio of actual evapotranspiration to precipitation.

2.3.2 Water conservation supply assessment model

Water conservation (*WC*) propelled by natural media such as water flow are one of the essential functions of ES. This research calculates the water conservation supply (*WCS*) (Guan et al., 2022) using the water yield section of the InVEST model:

$$WC = \min\left(1, \frac{249}{\text{Velocity}}\right) \times \min\left(1, \frac{0.9 \times TI}{3}\right) \times \min\left(1, \frac{K_{\text{soil}}}{300}\right) \times Y_x, \tag{2}$$

$$TI = \lg\left(\frac{\text{Watershed}}{\text{Soildepth} \times \text{Percentslope}}\right), \tag{3}$$

$$Y_{x,j} = \left(1 - \frac{AET_{x,j}}{P_x}\right) \times P_x, \tag{4}$$

where *WC* is water conservation (mm), Velocity is runoff coefficient, *TI* is the topographic index of topography, dimensionless. K_{soil} is soil saturation hydraulic conductivity (cm/d), *Y* is the water yield. Watershed is catchment raster data, dimensionless. Soildepth is soil depth (mm), Percentslope is the slope (percentage), $Y_{x,j}$ and $AET_{x,j}$ are the annual water yield (mm) and average

Table 1 Summary of the primary data

Data type	Data format	Resolution	Data sources
Land use/land cover	Raster	1 km	Resource and Environment Science and Data Platform
Precipitation	Raster	1 km	National Tibetan Plateau Data Center
Temperature	Spreadsheet	/	National Meteorological Science Data Center
Evapotranspiration	Raster	1 km	National Ecosystem Science Data Center
Soil data	Raster	30 arc-second	China soil map based harmonized world soil database (HWSD)
GDP	Raster	1 km	Resource and Environment Science and Data Platform
DEM	Raster	1 km	The National Tibetan Plateau Data Center
Population data	Raster	1 km	Resource and Environment Science and Data Center
Population economic data	Spreadsheet	/	China Statistical Yearbook, China City Statistical Yearbook
Water resources and food data	Spreadsheet	/	The Water Resources Bulletin of the YRB and South-west Rivers, the Yangtze River Yearbook
Energy data	Spreadsheet	/	The China Energy Statistics Yearbook

annual evapotranspiration (mm) of raster x on landscape type j, respectively. P_x is the annual precipitation (mm) of raster x.

2.3.3 Carbon sequestration supply assessment model

An alternate technique that uses library data to estimate carbon sequestration (CS) is the InVEST model (Wang et al., 2022a). The determination method of carbon density refers to previous studies (Pan et al., 2022; Ma et al., 2023), combined with the measured carbon density in the adjacent study area (Zou et al., 2021; Cao et al., 2022), after analyzing its rationality and screening outliers. The carbon sequestration supply (CSS) can be determined as follows:

$$C_{\text{tot}} = C_{\text{above}} + C_{\text{below}} + C_{\text{soil}} + C_{\text{dead}}, \tag{5}$$

where C_{tot} represents the total quantity of carbon stored in the region, C_{above} represents carbon stored above ground, C_{below} represents carbon stored in underground roots, C_{soil} represents carbon stored in the soil, and C_{dead} represents carbon stored in dead organic material.

2.3.4 Climate regulation supply assessment model

In this study, the total energy consumed by evapotranspiration of ecosystems was taken as the physical quantity of climate regulation (*CR*) in the YRB (Wang et al., 2023), and the alternative cost approach was utilized to assess the worth of *CR*. The climate regulation supply (*CRS*) was estimated using the intelligent urban ecosystem management system (IUEMS) (Peng et al., 2022). The supply of climate regulation can be calculated as follows:

$$E_{\text{tt}} = E_{\text{pt}} + E_{\text{we}}, \tag{6}$$

$$E_{\text{pt}} = \sum_i^n EPP_i \times S_i \times D \times 10^6/(3600 \times r), \tag{7}$$

$$E_{\text{we}} = E_{\text{w}} \times q \times 10^3/3600, \tag{8}$$

where E_{tt} denotes the amount of energy used for both evaporation and transpiration in an ecosystem (kWh/yr), E_{pt} denotes the energy consumed by ecosystem vegetation transpiration (kWh/yr), E_{we} denotes the amount of energy used for ecosystem water surface evaporation (kWh/yr), EPP_i denotes the amount of heat used for transpiration per unit area in the type i ecosystem (kJ·m^{-2}·d^{-1}), S_i denotes the area of the type i ecosystem (km^2), D denotes the open air-conditioning days, r is the energy efficiency ratio of the air conditioner: 3.0, dimensionless. i represents the ecosystem type, dimensionless, E_{w} denotes the amount of water that evaporates from the surface (m^3), and q represents the heat that is latent of volatilization, which is the heat required to vaporize 1 g of water (J/g). According to the IUEMS system, this paper determines that the number of days greater than 26°C per year is the number of days of air conditioning opening, and q is the latent heat of volatilization. The recommended value of this system is 2432.00 J/g (Zou et al., 2019). The raster data of land use types were reclassified into cultivated land, forest land, grassland, water area, unused land, and shrub land, and the daily transpiration heat consumption coefficient of different vegetation spaces recommended by the IUEMS system was adopted (Wang et al., 2023).

2.4 Construction of the ecosystem service demand assessment model

2.4.1 Freshwater supply service demand assessment model

Freshwater supply service demand (FSD) primarily emphasizes using water resources by human activities in production, life, and ecological space, disregarding the loss of vegetation absorption and utilization, river interception, and infiltration in natural hydrological processes (Deng et al., 2022). In this paper, the water consumption data of each department were used to allocate the water consumption at spatial positions based on the six land use types of grasslands, forestlands, cultivated land, construction land, water areas, and unused land (Chen et al., 2020). According to the land use data set of the YRB, the spatial distribution data of the various types of land uses in the YRB in 2010 and 2020 were extracted by using the Extract by Attributes function in ArcGIS. The water consumption can be calculated as follows:

$$\begin{aligned} W_{Ux} = & Wagr_x + Wind_x + Wdom_x + WLiv_x + Wgra_x \\ & + Wwland_x = A_x \times \text{Agr}_x + G_x \times Ind_x + P_x \times Dom_x \\ & + M_x \times Liv_x + C_x \times Gra_x + W_x \times Wwd_x, \end{aligned} \tag{9}$$

where $Wagr_x$ is the water consumption of agricultural irrigation in the YRB (m^3), A_x is the area of cultivated land in the YRB (km^2), and Agr_x is the average water consumption per mu of farmland irrigation in the YRB, which must be converted. $Wind_x$ is the industrial water consumption in the YRB, G_x denotes the GDP density data, with units of ten thousand yuan/km^2, Ind_x is the annual average water consumption of production per ten thousand yuan of the GDP in the YRB (m^3/ten thousand CNY), which is the domestic water consumption of urban and rural residents in the YRB, and P_x is the population density of the YRB, with units of person/km^2. Dom_x is the per capita comprehensive water consumption of urban and rural residents in the YRB, and the unit is m^3/person. $WLiv_x$ is the provincial livestock water consumption, M_x is the total number of livestock, and Liv_x is the annual average consumption of livestock in province x (m^3/head). $Wgra_x$ is the provincial grassland irrigation water consumption, C_x is the grassland area of the YRB, and Gra_x is the grassland irrigation water consumption

per unit area of the YRB. $Wwland_x$ is the amount of woodland irrigation water in the YRB, W_x is the woodland area of the YRB, and Wwd_x is the amount of woodland irrigation water per unit area of each province of the YRB. Table 2 displays the region-specific water usage indicators for the YRB. According to the land type water allocation table (Table 3), spatial discretization of the water use statistics in the YRB based on the spatial distribution map of the land use types can be realized, and water demand data with both the spatial geographical location and water consumption and administrative units can be obtained.

2.4.2 Water conservation demand assessment model

In this study, the water quota method (Yuan et al., 2023) was used to estimate the water conservation demand (WCD). Agriculture-related water, industrial water, residence water, animal water, and forest water were the five categories into which water usage was broken down. The Water Resources Bulletin of the YRB was used to determine domestic and industrial water consumption, and the water quotas of the provinces were used to determine the water consumption for agriculture, animal husbandry, and forestry. Finally, the spatial distribution of the water conservation requirement was determined by combining the grid density of the population, GDP density, and cultivated land data. The water conservation service demand can be calculated as follows:

$$D(L_r) = BE_r + F_r + G_r + BJ_r + W_r, \tag{10}$$

where L_r is the total water consumption of water unit r, BE_r is the farmland water consumption of water unit r, F_r denotes the industrial water consumption of water unit r, G_r is the domestic water consumption of water unit r, BJ_r denotes the animal water consumption of unit r, and W_r is the total amount of woodland water used by water unit r.

2.4.3 Carbon sequestration demand assessment model

The need for CS was estimated using the selected carbon emission coefficient in this research. The regional distribution of the carbon sequestration demand (CSD) was represented using data on energy statistics per individual carbon output and administrative units (Xue et al., 2022), as follows:

$$C_e = \sum_{i=1}^{n} P_i \times \varphi, \tag{11}$$

where C_e is the total carbon emissions (t/yr), P_i is the population of the ith village, and φ is the per capita carbon emissions (t/yr). The per capita carbon emission data were calculated by the energy consumption of the provinces of the YRB, using the carbon emissions provided by the IPCC in the Guidelines for National Greenhouse Gas Emission Inventories.

Table 2 Water consumption index of provinces in the Yangtze River Basin

Region	Number of large livestock by the end of the year/$\times 10^4$	Daily drinking water/ ($L \cdot head^{-1} \cdot d^{-1}$)	Woodland/ ($m^3 \cdot acre^{-1}$)	Grassland irrigation/ ($m^3 \cdot acre^{-1}$)
Shanghai	6.8	67	90	0
Jiangsu	40.9	55	100	0
Zhejiang	19.9	45.2	75	75
Anhui	151.5	60	70	0
Fujian	70.2	40	75	0
Jiangxi	277.1	37	75	0
Henan	1044.8	42	180	0
Hubei	327.5	45	107.14	0
Hunan	440.3	67	96.2	186
Guangdong	229.3	57	926	588
Guangxi	495.6	70	321	100
Chongqing	131.4	80	195	0
Sichuan	1085	53	242	0
Guizhou	627.6	33.75	173	80
Yunnan	923.1	35	95	146
Xizang	662.2	50	0	0
Shaanxi	186.4	51	226.5	370
Gansu	595	60	130	220
Qinghai	485.7	40	300	175

Table 3 Water allocation table of land type

Land use type	Corresponding water classification
Cultivated land	Agricultural irrigation water for wheat, corn, rice, barley, etc.
Woodland	Orchards, shrubs and other irrigation water
Grass land	Livestock grazing (sheep, cattle, etc.)
Waterbody	Fishery breeding
Urban construction land	Urban and rural domestic water, industrial production water
Unutilized land	Undistributed

2.4.4 Climate regulation demand assessment model

CR not only provide the benefits of offsetting anthropogenic carbon emissions but also provide a wide range of indirect and direct effects. This study regards agricultural production as a benefit (Wu et al., 2011). The reduced water consumption, reduced crop yield, rainstorm days and high-temperature days were used to calculate the climate regulation demand (CRD). According to the Yangtze River Yearbook and the Water Resources Bulletin of the YRB and south west Rivers, the reduction in grain production and the reduction in available water in the YRB in 2000, 2010, and 2020 were counted. The number of rainstorm days and high-temperature days in the YRB in one year were expressed as an indicator of the increased flood risk and an indicator of the increased heat stroke mortality, respectively (Serna-Chavez et al., 2014). These four types of data indicators were normalized. The CR_d can be calculated as follows:

$$CR_d = N_{(i,\text{decrease})} + W_{(i,\text{decrease})} + D_{(i,\text{decrease})} + M_{(i,\text{decrease})}, \quad (12)$$

where CR_d is the demand for CR, $N_{(i,\text{decrease})}$ is the reduced crop yield, $W_{(i,\text{decrease})}$ denotes the reduced available water consumption, $D_{(i,\text{decrease})}$ is the increased flood risk, and $M_{(i,\text{decrease})}$ is increased heat stroke mortality. According to the Yangtze River Yearbook and the Yangtze River Basin and South-west Rivers Water Resources Bulletin, the grain yield reduction and available water reduction in the Yangtze River Basin in 2000, 2010, and 2020 were counted. The number of rainstorm days and high-temperature days in the YRB every year represents the indicators of increased flood risk and heatstroke mortality, and these four types of data indicators are normalized.

2.5 Construction of the ecosystem service flows assessment model

Ecosystem service flow is expressed in this research as the gap between the production and consumption of ES. The freshwater supply service flow (*FSF*), water conservation service flow (*WCF*), carbon sequestration service flow (*CSF*) and climate regulation service flow (*CRF*) are calculated by a grid calculator as follows:

$$ES_i = ESS_i - ESD_i, \quad (13)$$

where ES_i is the ecosystem service flow of the 1-km grid i and ESS_i and ESD_i are the service supply and demand, respectively of grid i. Before calculating the flow of CR, the supply and demand of climate regulation services must be normalized (value range: 0−1).

The supply-demand ratio for ES provides insight into the connection between these two factors (Meng et al., 2021). The supply–demand ratio can be calculated as follows:

$$ESDR = \frac{S - D}{(S_{\max} + D_{\max})/2}, \quad (14)$$

where $ESDR$ is the supply–demand ratio of ES and S and D are the supply and demand of ES, respectively. $S_{\max}$ and $D_{\max}$ are the maximum values of the supply and demand, respectively.

The comprehensive supply and demand ratio of ecosystem services (*CESDR*) indicates ecosystem service status by integrating the supply and demand of numerous ES (Liu et al., 2022a). *CESDR* can be calculated as follows:

$$CESDR = \frac{1}{n}\sum_{i=1}^{n} ESDR_i, \quad (15)$$

where n is the number of ES, $n = 4$, and $ESDR_i$ is the supply–demand ratio of the various types of ES.

3 Result

3.1 Spatial differentiation analysis of the ecosystem service supply

The total supply of *FS* in 2000, 2010, and 2020 was 7.03×10^{11} m^3, 8.56×10^{11} m^3, and 10.97×10^{11} m^3, respectively (Fig. 5(a)). The average water supply depths in the whole basin were 478.95 mm, 642.84 mm, and 787.09 mm, respectively. The maximum water supply depths in the whole basin were 2234.88 mm, 2553.54 mm, and 2465.88 mm, respectively (Fig. 2(a)). Water yield increased from north-west to south-east due to precipitation and ecological types. The sections of the YRB with the highest water yield per unit area were mainly situated in the center and south-east. On the one hand, this area exhibits abundant rainfall and low potential evapotranspiration. On the other hand, due to the dense water network, low mountain basins and wide plains in this area, the altitude is low, the soil is fertile, and the catchment volume is high, so the fresh water supply capacity is high. The low-value areas of the water yield per unit area were mainly located in the north-west. The vegetation coverage in this area is high, the altitude is

high, and mostly high mountain areas occur. Low soil and groundwater reserves diminish the water supply capability of this region.

In 2000, 2010, and 2020, the YRB could save up to 800.21 mm, 1146.21 mm, and 894.51 mm of water (Fig. 2(b)). The total amount of water saved was 15077 billion m^3, 17848 billion m^3, and 23381 billion m^3, respectively (Fig. 5(d)). The supply of *WC* exhibited a decreasing and then increasing tendency from the south-west to the north-east. Climatic conditions, topography, and human activity density primarily influence the spatial variation in water conservation within the basin. East and south-west of the basin comprised the majority of the high-value areas. The area exhibits high precipitation, large forestland area and high soil water content, so the water conservation capacity is high. Low-value areas were mainly in the north-west and center. On the one hand, the precipitation in this area is less than that in the lower reaches of the basin, and the vegetation transpiration ability is high. On the other hand, the potential for water conservation in this region is inadequate due to the high population density and the expansion of the agricultural and building land areas.

The total carbon sequestration of the YRB ecosystem in 2000, 2010, and 2020 was 18.043 billion tons, 17.985 billion tons, and 17.957 billion tons, respectively (Fig. 5(g)). The supply of *CS* showed a gradual downward trend. *CS* have had a stable regional distribution for 20 years (Fig. 2(c)). East and south of the basin, where forest cover is high, are where *CS* are most assertive, while the north-western desert region and the area with the highest urbanization rate are where they are weakest.

In 2000, 2010, and 2020, ecosystem transpiration and evaporation in the YRB consumed 3.68×10^{13} kWh, 3.19×10^{13} kWh, and 3.73×10^{13} kWh, respectively (Fig. 5(i)). The economic value of *CR* in the YRB based on the grid units in 2000, 2010, and 2020 ranged from 11.13−214.53 kWh/m^2, 9.96−164.83 kWh/m^2, and 11.13−183.63 kWh/m^2, respectively (Fig. 2(d)). The economic values of *CR* in the YRB based on the grid units in 2000, 2010, and 2020 were 4.78−92.25 CNY/m^2, 5.28−87.36 CNY/m^2, and 5.67−93.66 CNY/m^2, respec-

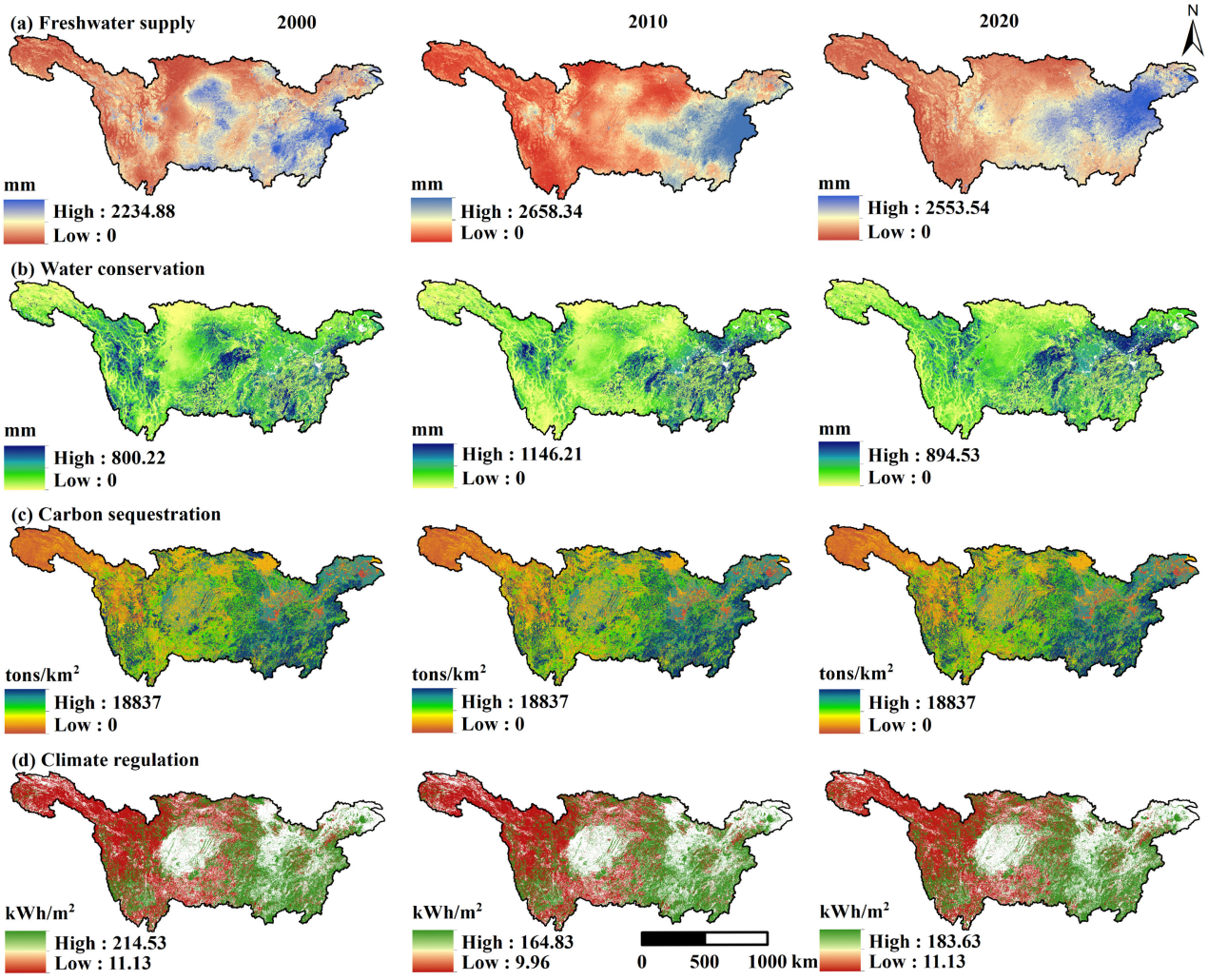

Fig. 2 Ecosystem service supply in the YRB in 2000, 2010, and 2020.

tively, and their total values were 15.84 trillion CNY, 16.88 trillion CNY, and 19.03 trillion CNY, respectively. In the YRB, there was a tendency to first reduce and then raise the supply for *CR*. The spatial distribution pattern of the climate regulation supply function significantly changed. The region with the highest supply of *CR* was located in the eastern portion of the basin. In contrast, the part with the lowest capacity for *CR* was situated in the western portion.

3.2 Spatial differentiation analysis of the ecosystem service demand

The total demand for *FS* in the YRB in 2000, 2010, and 2020 was 176.409 billion m^3, 173.131 billion m^3, and 157.193 billion m^3, respectively (Fig. 5(b)). The demand for *FS* in the YRB is gradually decreasing. From the spatial pattern analysis, towns and industries are densely distributed in the central and south-eastern parts of the YRB, and the water demand is much higher than that in the north-western and north-eastern parts of the basin (Fig. 3(a)). The region with the lowest water demand is concentrated north-west of the basin. The land cover type in this area is mainly grassland, which is sparsely populated and has a lower water demand for human production activities.

In 2000, 2010, and 2020, *WC* matched *FS* in quantity and space. In 2000, 2010, and 2020, the *WCD* of the YRB reached 6.89×10^{10} m^3/km^2, 6.82×10^{10} m^3/km^2, and 6.37×10^{10} m^3/km^2, respectively (Fig. 3(b)). The average demand for *WC* in the YRB from 2000 to 2020 was 9.28×10^8 m^3, 9.11×10^8 m^3, and 8.27×10^8 m^3, respectively (Fig. 5(e)). The water demand in the YRB is generally high in the middle and low around. Additionally, the eastern basin of Sichuan and the eastern plain of Hubei were the areas with the highest demand for *WC*, the southern region of Qinghai Province had the lowest request.

In 2000, 2010, and 2020, the total carbon demand in the YRB was 4.05×10^8 tons, 1.12×10^9 tons, and 1.23×10^9 tons, respectively (Fig. 5(h)). The total carbon demand exhibited an upward trend, with an increased rate of

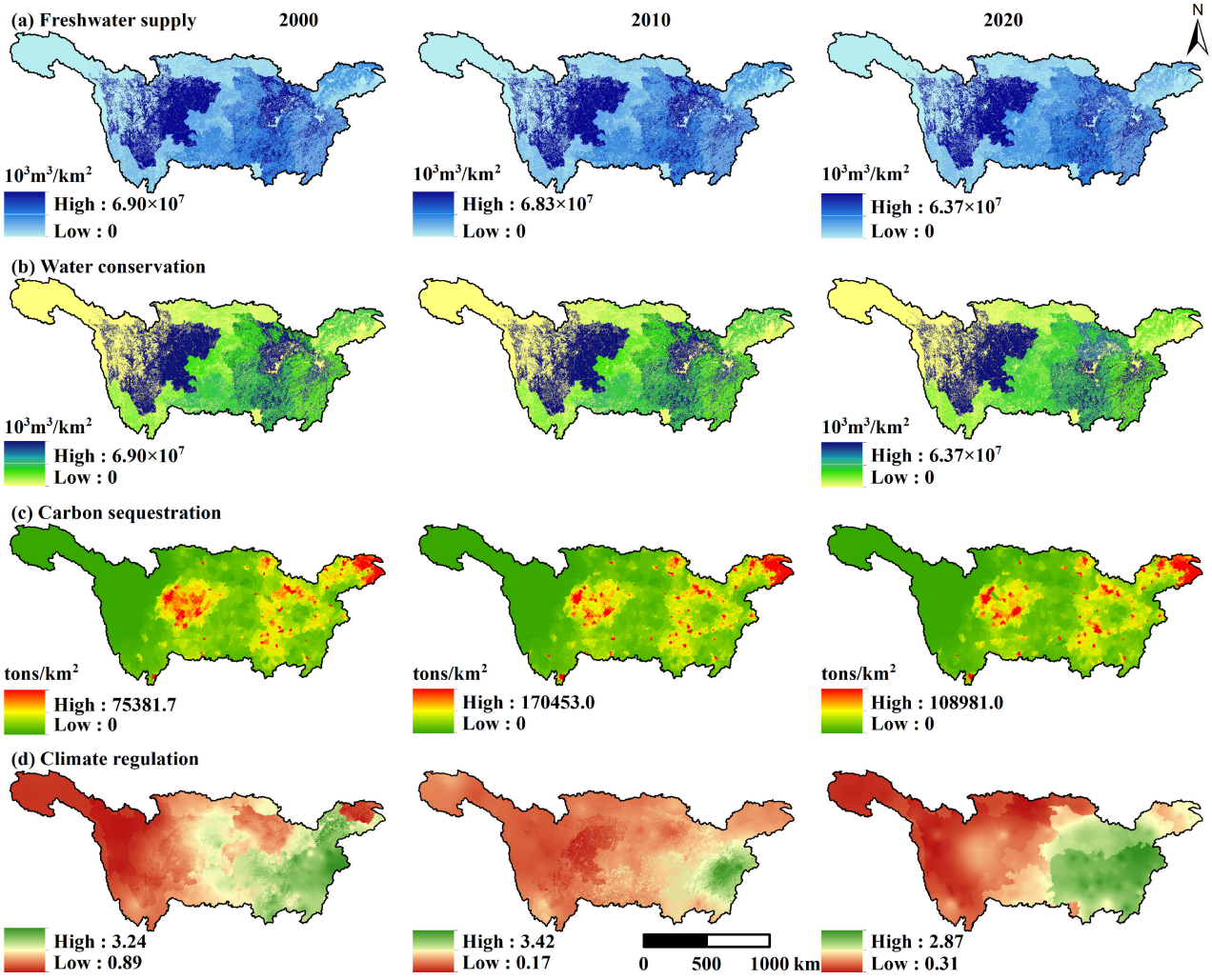

Fig. 3 Ecosystem service demand in the YRB in 2000, 2010, and 2020.

204.62%. In 2000, 2010, and 2020, the total carbon emissions in the YRB were 738 million tons, 2.315 billion tons, and 2.574 billion tons, respectively. In 2000, 2010, and 2020, the per capita carbon emissions in the YRB were 0.94 tons/person, 2.49 tons/person, and 2.58 tons/person, respectively. The total carbon emissions and per capita carbon emissions showed upward trend, and the increase rates were 248.68% and 173.89%, respectively. In 2000, 2010, and 2020, the demand for *CS* per unit area in the YRB reached 7.54×10^4 tons/km^2, 1.70×10^5 tons/km^2, and 1.09×10^5 tons/km^2, respectively (Fig. 3(c)). There was a rising demand for *CS*. Each year, the appetite for *CS* per unit area exhibited a distinct spatial variation. As shown in Fig. 4, in the central and eastern parts of the region, the high-value locations of the *CSD* were point-like, whereas, in the north-eastern part, they were block-like. The area is mainly a population gathering area and an industrial area with high carbon emissions. The region with the lowest demand for *CS* is situated north-west of the basin, with minimal population density.

The climate regulation service demand index values based on the grid units in 2000, 2010, and 2020 ranged from 0.89 to 3.24, 0.17−3.42, and 0.31−2.87, respectively (Fig. 3(d)). The climate regulation service demand index of the YRB in 2000, 2010, and 2020 was 1.93, 1.22, and 1.23, respectively (Fig. 5(j)). The spatial heterogeneity is phenomenal, and there was a tendency in the YRB toward first falling and then increasing requirements for *CR*. The entire distribution pattern is high in the east and low in the west, with the high value expanding at first and then shrinking progressively. The appetite for *CR* in the watersheds of Hunan, Hubei, and Jiangxi provinces changed substantially, whereas it was low in the regional north-west.

3.3 Spatial differentiation analysis of ecosystem service flows

The total *FSF*s of the YRB ecosystem in 2000, 2010, and 2020 were −176.425 billion m^3, −173.148 billion m^3, and −157.202 billion m^3, respectively. The *FSF* per unit area

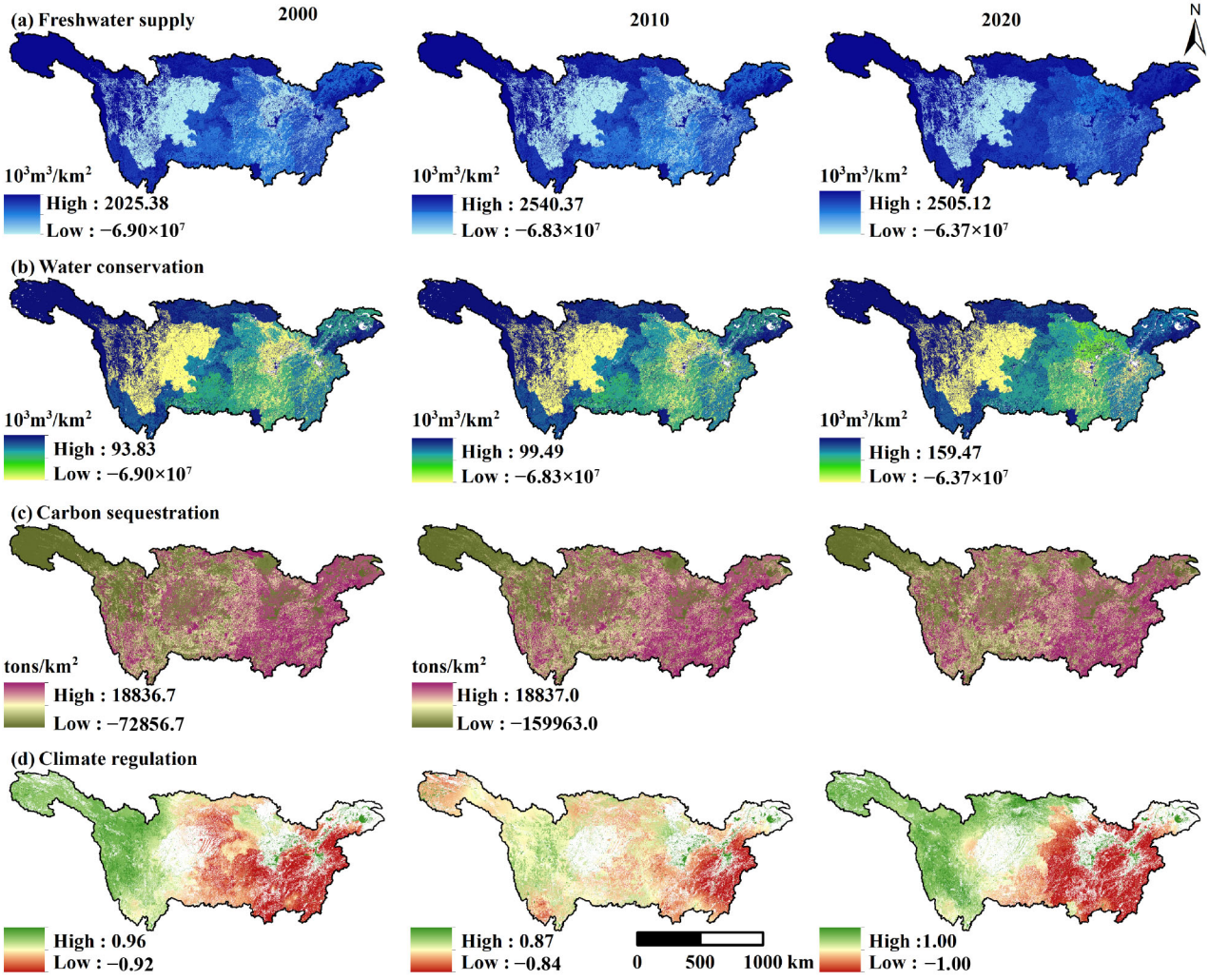

Fig. 4 Ecosystem service flows in the YRB in 2000, 2010, and 2020.

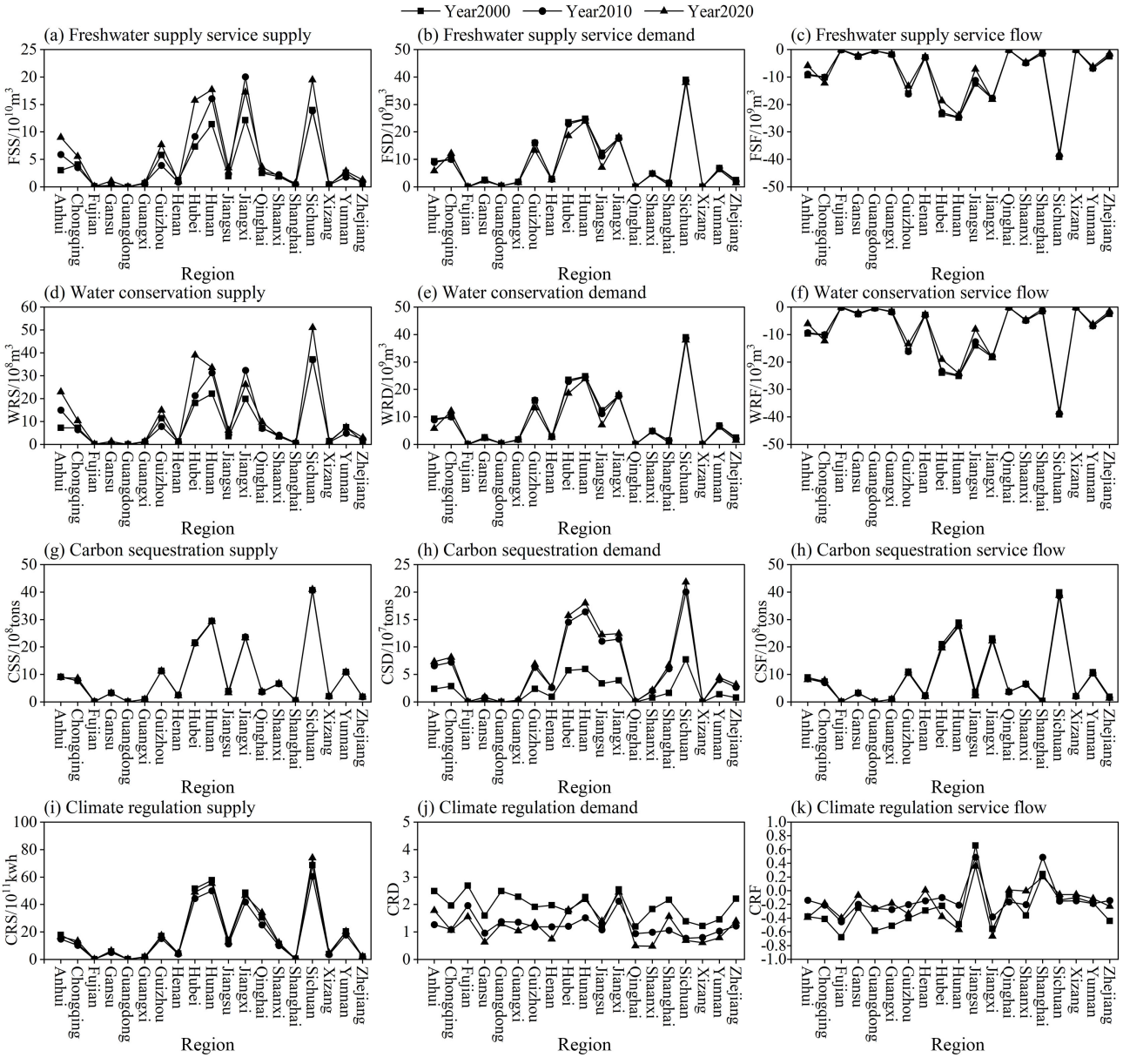

Fig. 5 The supply, demand and flow of ecosystem services at the provincial scale of YRB.

in 2000, 2010, and 2020 reached 2025.38 × 10^3 m^3/km^2, 2540.37 × 10^3 m^3/km^2, and 2505.12 × 10^3 m^3/km^2, respectively. The service flow of *FS* in the YRB generally showed a decreasing trend and indicated a distribution pattern comprising low levels in the middle and high values around (Fig. 4(a)). The *FSF*s were oversupplied in the north-west and north-east of the basin and were in short supply in the eastern upstream region of the basin.

The total *WCF*s of the YRB ecosystem in 2000, 2010, and 2020 were −179.508 billion m^3, −176.095 billion m^3, and −159.563 billion m^3, respectively. The water conservation flow per unit area in 2000, 2010, and 2020 reached 93.83 × 10^3 m^3/km^2, 99.48 × 103 m^3/km^2, and 159.47 × 10^3 m^3/km^2, respectively (Fig. 4(b)). Water conservation services were generally in short supply, and the service flow of *WC* showed a gradual downward trend, with obvious spatial differentiation.

The total *CSF*s of the YRB ecosystem in 2000, 2010, and 2020 were 17.635 billion tons, 16.859 billion tons, and 16.723 billion tons, respectively. In 2000, 2010, and 2020, the *CSF* per unit area reached 18837 tons/km^2, and the lowest *CSF*s per unit area were −72856.7 tons/km^2, −159963 tons/km^2, and −106456 tons/km^2, respectively (Fig. 4(c)). Carbon sequestration services were generally in a state of oversupply, and the service flow of *CS* gradually decreased. The land cover types in the north-west of the basin mostly include grassland, and the carbon demand is low, so the *CSF* in the area is low. Due to the high population density and predominance of cultivated land in the south-east of the basin, the *CSF* is

substantial in this region.

The average index values of the *CRF* in 2000, 2010, and 2020 were −0.271, −0.136, and −0.175, respectively. The index values of the *CRF* based on the grid units in 2000, 2010, and 2020 ranged from −0.92 to 0.96, −0.84 to 0.87, and −1.00 to 1.00, respectively (Fig. 4(d)). Climate regulation services were generally in short supply, and the *CRF* showed a trend of declining and then growing. The low-value areas to the south-east first contracted and then expanded and greatly fluctuated during the period, which is mainly related to rainfall and evapotranspiration in the basin. The north-west of the basin exhibits high vegetation coverage and a low demand for *CR*, so the regional *CRF* is high.

3.4 Dynamic change analysis of ecosystem service flows

From 2000 to 2020, the average annual *FSF* in the YRB was 168.925 billion m^3. Moreover, Sichuan and Hunan attained the highest *FSF*, with an average annual *FSF* of more than 24.4 billion m^3, and the lowest average annual *FSF*s were observed in Xizang and Fujian, both less than 99 million m^3 (Fig. 5(c)). Figure 5 shows that there is a large gap in the *FSF* among the various administrative regions. Overall, the *FSF* in the central inland area is much lower than that in the surrounding river and sea areas, which is positively correlated with the spatial distribution position of water resources and population density. From 2000 to 2020, the provinces with the largest changes in the annual average *FSF*s were Jiangsu and Hubei. In 2000, 2010, and 2020, the total *FSF* in the YRB greatly changed and showed a gradual downward trend, reaching 176.425 billion m^3, 173.148 billion m^3, and 157.202 billion m^3, respectively.

From 2000 to 2020, the average yearly *WCF* in the YRB was 171.722 billion m^3. Among the various units, Sichuan and Hunan attained the highest supply and demand flows of water conservation, with an average yearly *WCF* of more than 24.6 billion m^3. The lowest average yearly *WCF*s occurred in Xizang and Fujian, both less than 100 million m^3 (Fig. 5(f)). As shown in Fig. 5, the distribution of *WCF* among the various administrative areas has a significant discrepancy. Due to the geography and soil types, the *WCF* in the south-east coastal areas is often higher than in the interior western regions. The provinces with the largest changes in the three years were Jiangsu and Hubei. In 2000, 2010, and 2020, the total *WCF* in the YRB changed greatly and showed a gradual downward trend, reaching 179.508 billion m^3, 176.095 billion m^3, and 159.563 billion m^3, respectively.

From 2000 to 2020, the average annual *CSF* in the YRB was 17.072 billion tons. Among the various administrative units, Sichuan and Hunan had the highest *CSF*s, with an average annual *CSF* of more than 2.7 billion tons, and the lowest annual *CSF*s occurred Guangdong and Fujian, both less than 0.15 billion tons (Fig. 5(h)). There is a large gap in the *CSF* among the administrative regions. Overall, the *CSF* in the eastern part of the basin is much higher than that in the north-west region, which is positively correlated with the per capita carbon emissions and GDP. In 2000, 2010, and 2020, the total *CSF* in the YRB changed slightly and showed a gradual downward trend, reaching 17.635 billion tons, 16.859 billion tons, and 16.723 billion tons, respectively.

From 2000 to 2020, the average annual index of the *CRF* in the YRB was −0.599. Among the different regions, Jiangxi had the highest average annual index of the *CRF*, and the average annual index of the *CRF* was higher than 0.530. The lowest average annual index was observed in Qinghai, and the average annual index was lower than 0.070 (Fig. 5(k)). The gap in the index of the *CRF* among the various administrative regions is small. Overall, the climate regulation service in the YRB is in short supply, and the *CRF* in the south-east coastal area is higher than that in the western part of the basin, which is related to rainfall and evapotranspiration. The average index of the YRB in 2000, 2010, and 2020 greatly changed, showing a trend of first decreasing and then increasing, at −0.271, −0.136, and −0.175, respectively.

4 Discussion

4.1 Spatial-temporal differentiation analysis of ecosystem service flows at the watershed scale

Based on the provincial-scale service flow in the YRB, the quantitative changes in ecosystem service flows in the upper, middle and lower reaches are analyzed, as shown in Fig. 6. From 2000 to 2020, the *FSF* (Fig. 6(a)), *WCF* (Fig. 6(b)), and *CRF* (Fig. 6(d)) in the upper reaches of the Yangtze River (URYR) showed a gradual upward trend, and the *CSF* (Fig. 6(c)) showed a pattern that increased before diminishing. The average annual *FSF* and *WCF* in the URYR were −21.591 billion m^3 and −21.694 billion m^3, respectively. The average annual *CSF* was 7.610 billion tons, and the average annual index of the *CRF* was −0.143. The *FSF* and *WCF* in the middle reaches of the Yangtze River (MRYR) showed an upward trend, the *CSF* showed a decreasing trend, and the *CRF* exhibited an upward and then a decreasing trend. The average annual *FSF* and *WCF* in the MRYR were −18.611 billion m^3 and −18.825 billion m^3, respectively. The average annual *CSF* reached 8.181 billion tons, and the average annual index of the *CRF* was −0.372. The *FSF* and *WCF* in the lower reaches of the Yangtze River (LRYR) showed an upward trend, the *CSF* showed a gradually decreasing trend, and the *CRF* showed a trend of first increasing and then decreasing. The average annual *FSF* and *WCF* in the LRYR were −8.436 billion m^3 and −8.924 billion m^3, respectively. The average annual *CSF* was 1.281 billion tons, and the average

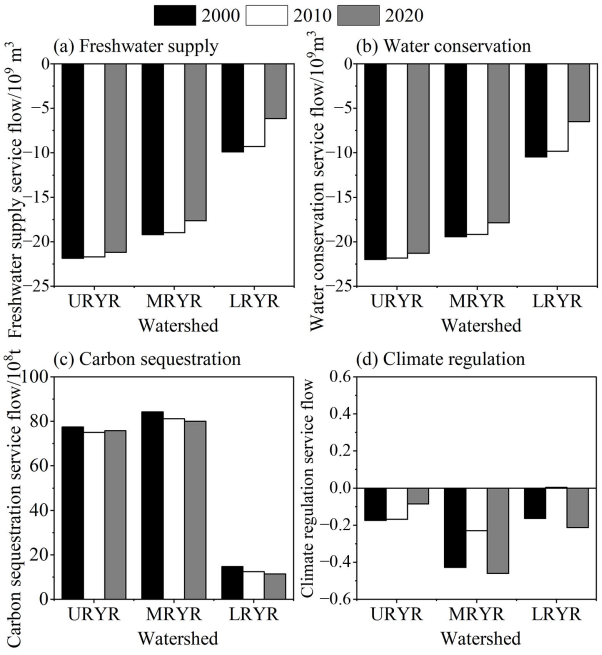

Fig. 6 The flow of ecosystem services at the watershed scale of YRB.

annual index of the *CRF* was −0.124.

The ecosystem service flows in the upper, middle and lower reaches of the YRB were quantitatively compared and analyzed. The *FSF* (Fig. 6(a)) and *WCF* (Fig. 6(b)) in the URYR were the highest, followed by the middle reaches and the lower reaches. The *CSF* in the MRYR was the highest, followed by the upstream and downstream reaches (Fig. 6(c)). The *CRF* was most extraordinary in the middle reaches, then the upper reaches, and finally the lower reaches (Fig. 6(d)).

The spatial differentiation of the ecosystem service flows in the upper, middle and lower reaches of the YRB is significant, as shown in Fig. 7 to Fig. 10. From 2000 to 2020, the *FS* (Fig. 7(a)) and *WC* (Fig. 8(a)) were most valuable in the north-eastern portion of the middle and lower reaches of the watershed. Most high-value regions are situated in the eastern portions of Sichuan Province, Hunan Province, Anhui Province, and Zhejiang Province. In contrast, the majority of the low-value areas are found in Qinghai Province and Chongqing City. The value-added *CSF* was significantly dispersed in its regional distribution from 2000 to 2020 (Fig. 9(a)). The more prominent high-value areas were located in the south-east of Chongqing, and the low-value areas were evenly distributed across the YRB. The spatial differentiation of the *CRF* in the upper, middle and lower reaches of the YRB was the most significant (Fig. 10(a)). From 2000 to 2020, the value-added areas of the *CRF* were mainly in the higher reaches of the basin, less in the middle and lower reaches, and least in the center. Among them, the more prominent low-value areas included Hunan

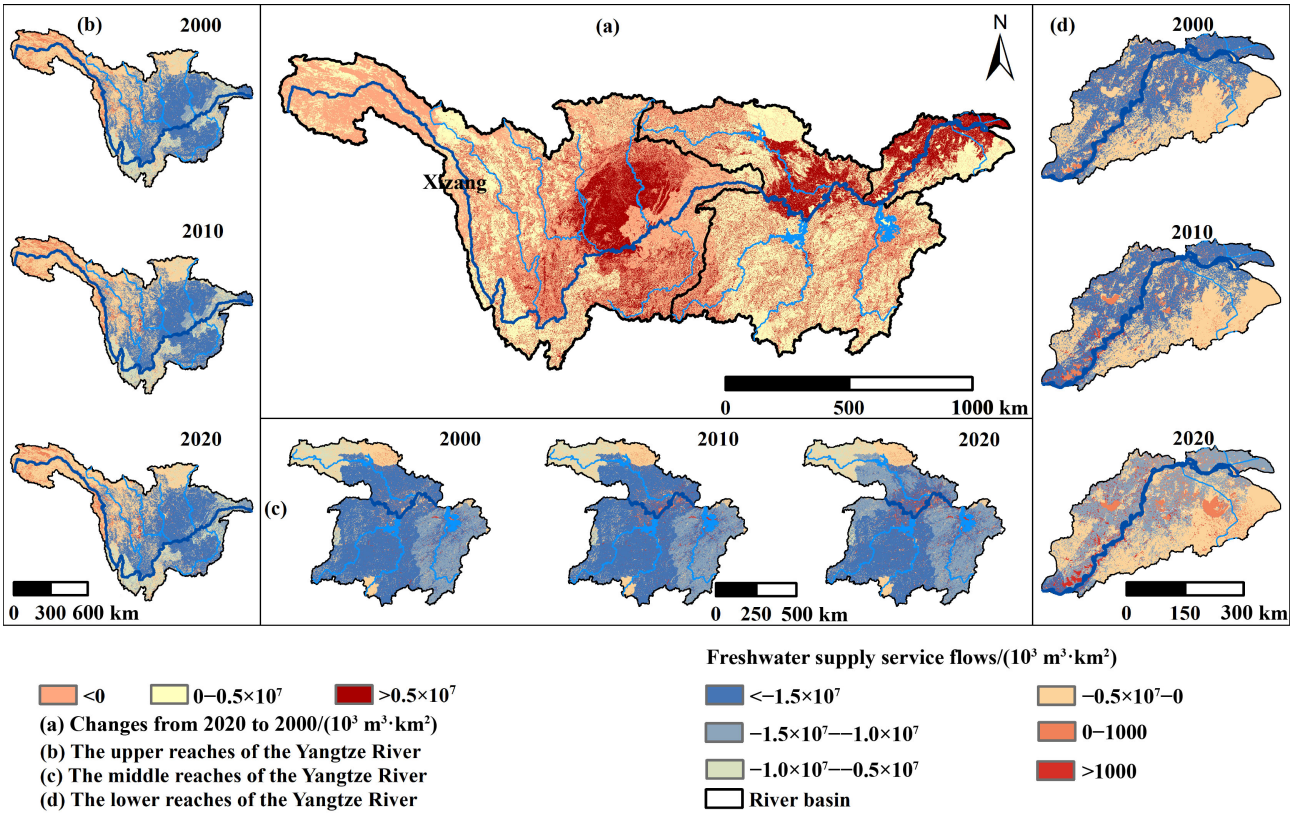

Fig. 7 The division of the upper, middle and lower reaches of the YRB and freshwater supply service flows in different provinces.

Province, Hubei Province, and Jiangxi Province.

From 2000 to 2020, the *FSF* in the YRB was generally in short supply. The high-value area of the *FSF* in the downstream basin gradually expanded downward as a block distribution (Fig. 7(d)). In contrast, the spatial distribution in the south-eastern part (Fig. 7(b)) and middle reaches of the upstream basin (Fig. 7(c)) remained stable. In addition, the *FSF* along the main stem of the Yangtze River was predominantly in a state of oversupply, especially the spatial differentiation of the high-value area of the *FSF* in the LRYR (Fig. 7(d)), which was significant.

From 2000 to 2020, the water conservation service in the YRB was in short supply. While the *WCF* in the upper reaches revealed a stable spatial distribution (Fig. 8(b)), the flow in the middle reaches showed a slow upward trend to the east (Fig. 8(c)), and the flow in the lower reaches exhibited an increasing tendency to the south (Fig. 8(d)).

From 2000 to 2020, Fig. 9 demonstrates that the carbon sequestration service in the YRB generally followed an oversupply trend. The capacity to provide *CS* was lowest in the upstream basin (Fig. 9(b)), whereas intermediate and low downstream basins had similar capabilities. The low-value area of the *CSF* in the upstream basin was located in the north-west, showing a decreasing trend eastward. The low-value area of the *CSF* in the middle reaches of the basin was distributed in a scattered manner (Fig. 9(c)), showing a gradual increasing trend to the east. In the downstream basin, the low-value area of the *CSF* exhibited irregularly increasing and decreasing blocks (Fig. 9(d)).

From 2000 to 2020, the *CR* in the YRB was generally in short supply. The flow of *CR* in the upstream basin to the south-east exhibited a decreasing and increasing pattern (Fig. 10(b)). The middle and lower reaches of the flow of *CR* revealed an eastward tendency that initially increased and subsequently decreased. Among the various regions, the high-value area of the *CRF* in the YRB was distributed in the downstream basin, showing a gradually increasing trend from the downstream part to the LRYR (Fig. 10(d)), and the low-stakes area was mainly occurred in the southern part of the middle reaches (Fig. 10(c)).

From 2000 to 2020, the hydrological characteristics of the URYR were obvious: the gap was large, the *FSF* and *WCF* were the highest, the *CRF* gradually increased, and the *CSF* change was not obvious. The trend of ecosystem service flow changes in the MRYR and LRYR was consistent. Their *CRF* changes were very significant (Fig. 6). The spatial and temporal changes of ecosystem service flow in the YRB are related to the policy of Yangtze River protection (Fang et al., 2021; Sheng et al., 2022; Guan et al., 2023). In 2021, the action plan to support the

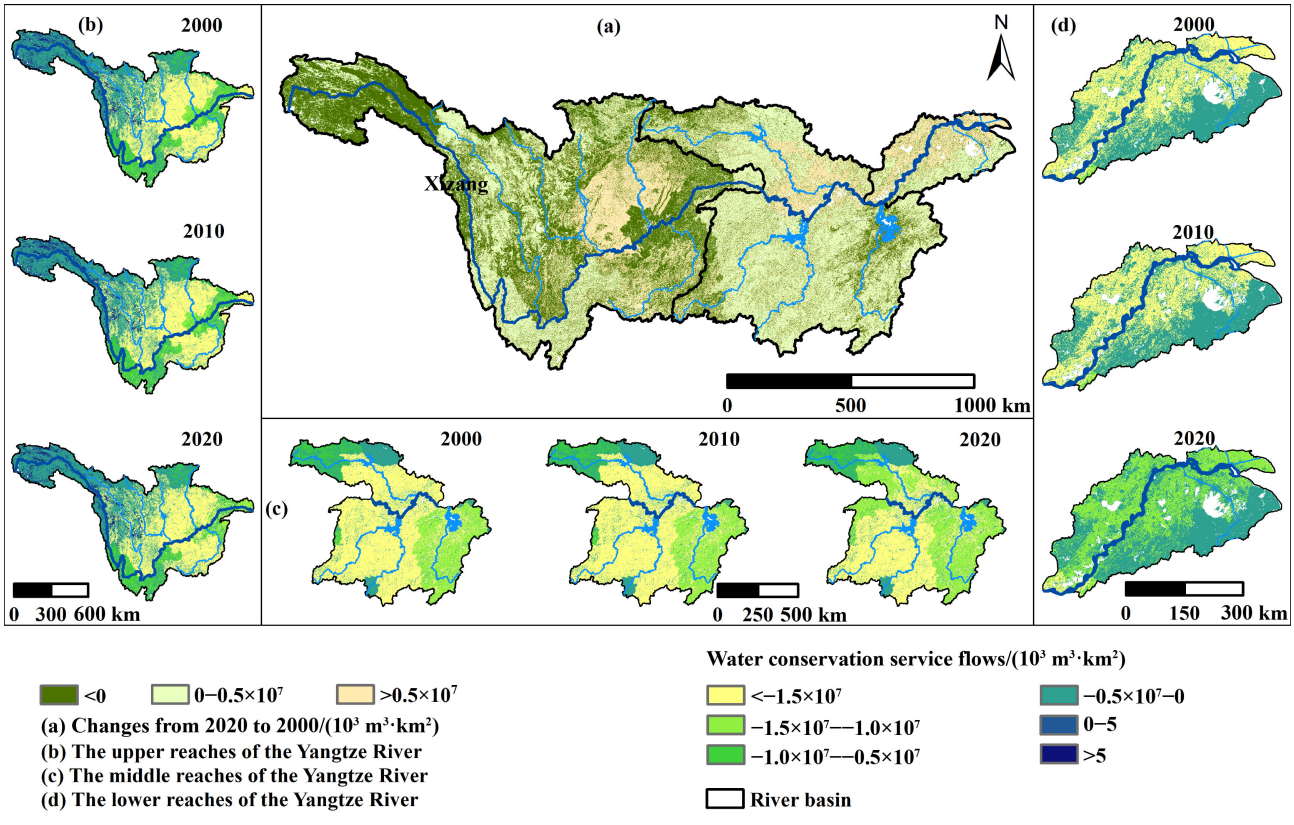

Fig. 8 The division of the upper, middle and lower reaches of the YRB and water conservation service flows in different regions.

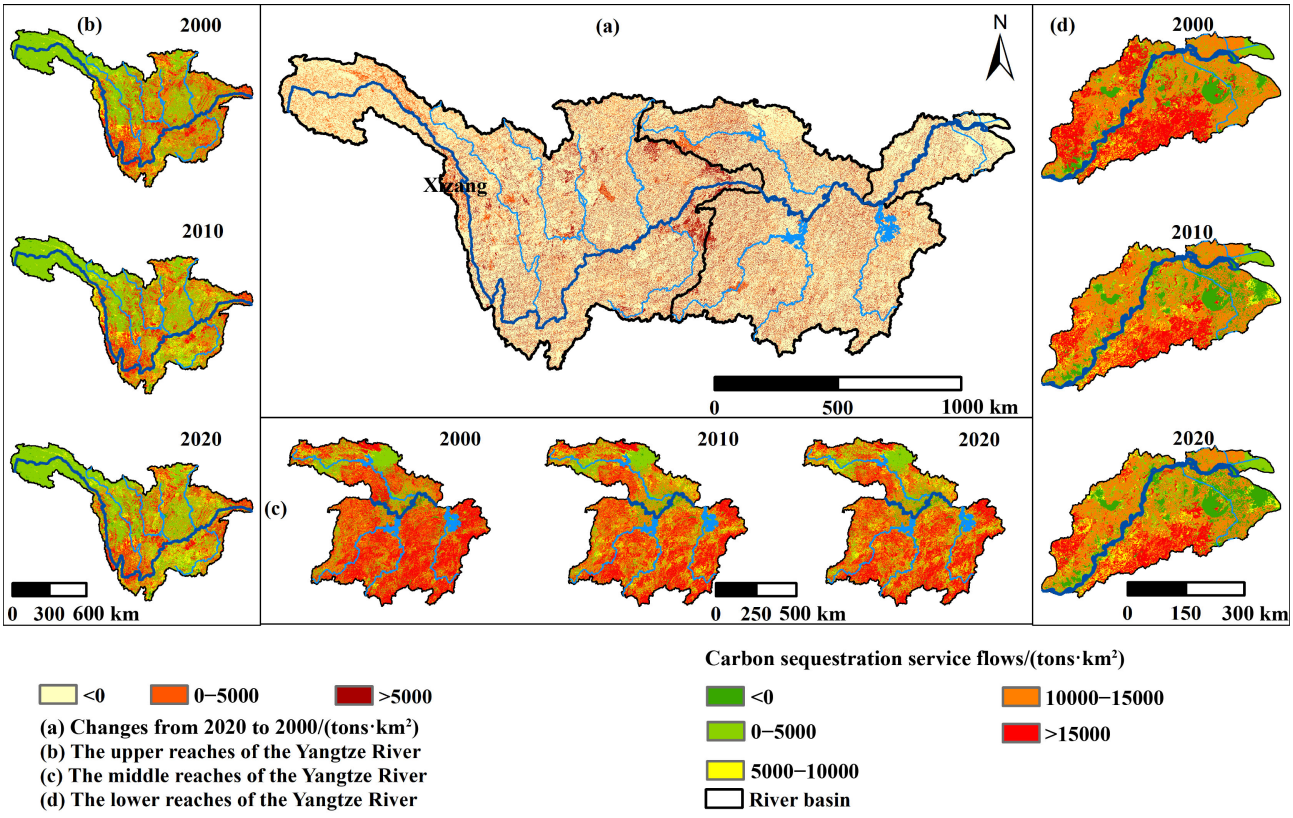

Fig. 9 The division of the upper, middle and lower reaches of the YRB and carbon sequestration service flows in different regions.

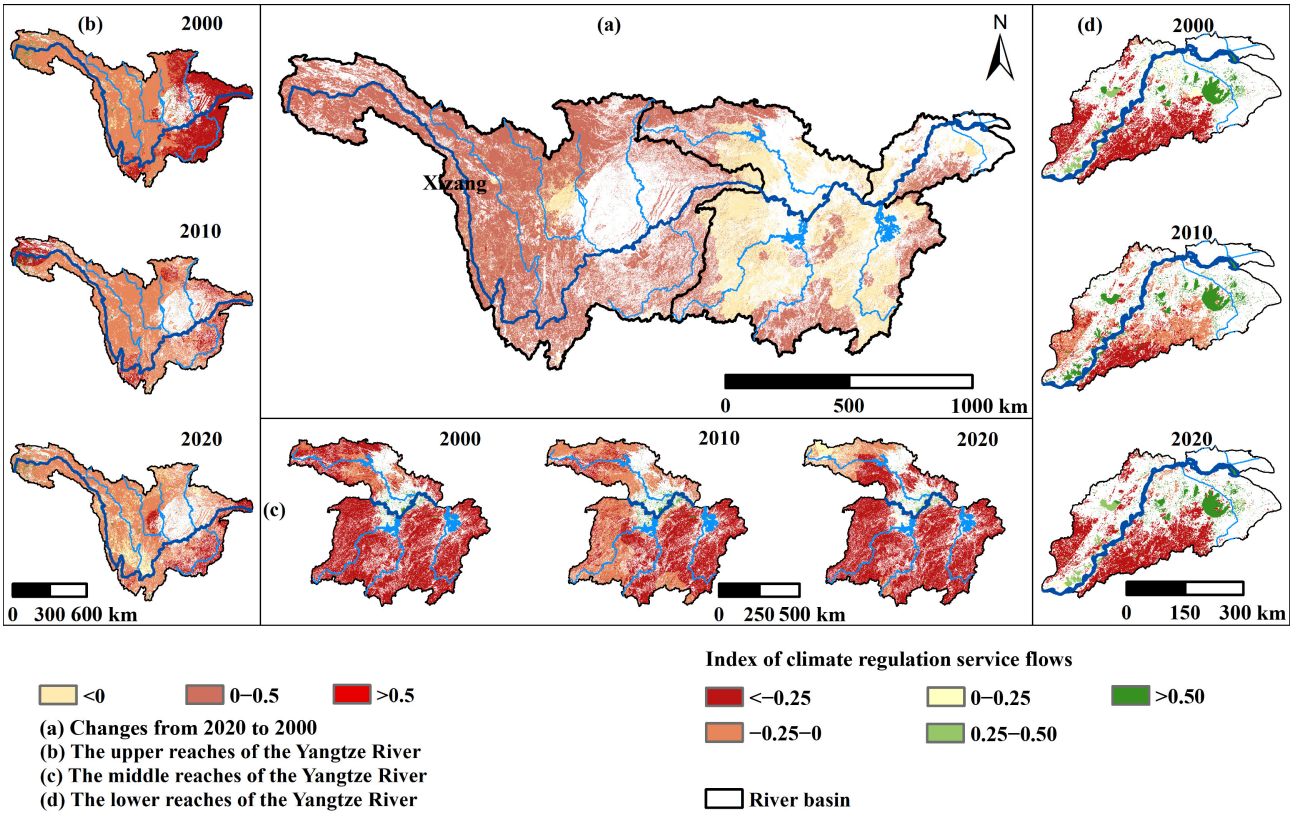

Fig. 10 The division of the upper, middle and lower reaches of the YRB and climate regulation service flows in different regions.

establishment of a horizontal ecological compensation mechanism in the YRB will be implemented, and the horizontal ecological compensation mechanism in the entire YRB will be established and improved to promote the Yangtze River Protection Plan (Sheng et al., 2022). The URYR bears the responsibility of protecting the ecological environment. The MRYR and LRYR could actively develop and adapt to local conditions and support the implementation of ecological environment restoration and other protection measures at the source and upper reaches of the YRB.

4.2 Spatial-temporal differentiation analysis of ecosystem service flows at the urban agglomeration scale

The urban agglomerations in the YRB include the CCUA, MRYRUA, and YRDUA. The ecosystem service flows in the different urban agglomerations are significantly different, as shown in Fig. 11. From 2000 to 2020, the *FSF* (Fig. 11(a)) and *WCF* (Fig. 11(b)) of the CCUA exhibited a gradual upward trend, and the *CSF* and *CRF* revealed decreasing and then rising trends, respectively. The average annual *FSF* and *WCF* of the CCUA were −40.948 billion m^3 and −41.078 billion m^3, respectively. The average annual *CSF* reached 2.143 billion tons, and the average annual index of the *CRF* is −0.262. The *FSF* and *WCF* of the MRYRUA exhibited an upward trend, the *CSF* exhibited a progressively decreasing trend (Fig. 11(c)), and the *CRF* exhibited an initial upward trend followed by a decreasing trend (Fig. 11(d)). The average annual *FSF* and *WCF* of the MRYRUA were −22.251 billion m^3 and −22.789 billion m^3, respectively. The average annual *CSF* reached 4.293 billion tons, and the average annual index of the *CRF* was −0.369. The *FSF* and *WCF* of the YRDUA observed an upward trend, the *CSF* revealed a gradually decreasing trend, and the *CRF* exhibited an upward and then a decreasing trend. The average annual *FSF* and *WCF* of the YRDUA were 7.968 billion m^3 and 8.451 billion m^3, respectively. The average annual *CSF* was 1.176 billion tons, and the average annual index of the *CRF* was 0.088. The ecosystem service flows of the CCUA, the MRYRUA, and the YRDUA were quantitatively compared and analyzed. As shown in Fig. 11, the YRB in the CCUA achieved the most extraordinary levels of the *FSF* and the *WCF*, followed by the MRYRUA and the YRDUA, respectively. The carbon sequestration service supply was most significant in the MRYRUA, followed by the CCUA, and lowest in the YRDUA. The *CRF* was most prominent in the MRYRUA, second highest in the CCUA, and minimal in the YRDUA.

The spatial differentiation of the ecosystem service flows in the urban agglomeration of the YRB is significant, as shown in Figs. 12−15. From 2000 to 2020, the high-value regions of the *FSF* (Fig. 12(a)) and the

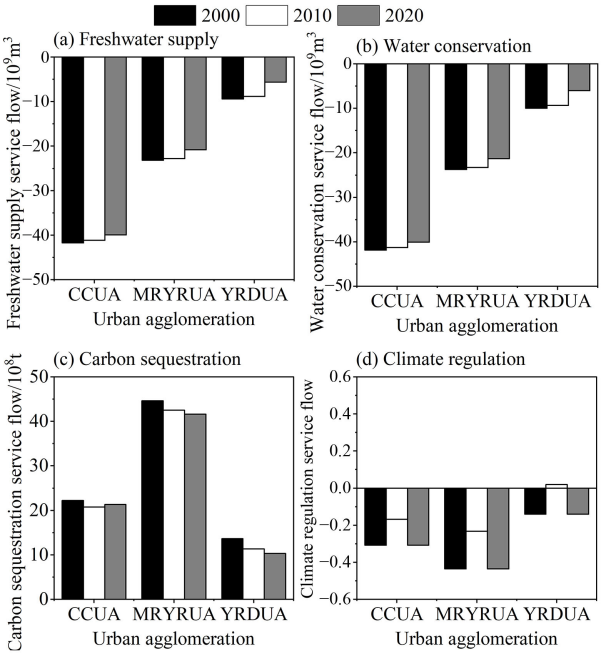

Fig. 11 The flow of ecosystem services at urban agglomeration scale of YRB.

WCF (Fig. 13(a)) were mainly in the west of the CCUA, the north of the MRYRUA, and the north-west of the YRDUA, while the low-stakes areas were in the east. Among the various urban agglomerations, the spatial differentiation of the *FSF* in the CCUA was the most significant (Fig. 12(a)). From 2000 to 2020, the change in the *CSF* in the urban agglomeration of the YRB was relatively gradual, and its value-added areas were scattered in the urban agglomeration in the form of aggregated points (Fig. 14(a)). The high-value area of the *CSF* was in the south-east part of the CCUA, and the low levels areas were spread out widely in the YRB urban agglomeration. From 2000 to 2020, the capacity of the *CRF* was reduced. The high-value regions were in the edge area of the CCUA, the central and south-eastern sections of the MRYRUA, and the southern area of the YRDUA, and the low levels areas were mainly in the MRYRUA (Fig. 15(a)).

From 2000 to 2020, the *FS* of the YRB urban agglomeration was in short supply, as shown in Fig. 12. The low-value area of the *FSF* in the CCUA gradually increases to the east, and the boundary between Sichuan and Chongqing presents the spatial dispersion pattern of east-high-west low (Fig. 12(b)). With a spatial dispersion pattern that includes high values in the north-east and low values in the south-west, the high-value region of the *FSF* in the MRYRUA steadily shrank from the edges to the center (Fig. 12(c)). The high-value region of the *FSF* in the YRDUA increased progressively to the south, exhibiting spatial dispersion with high levels in the south-east and low levels in the north-west (Fig. 12(d)). The

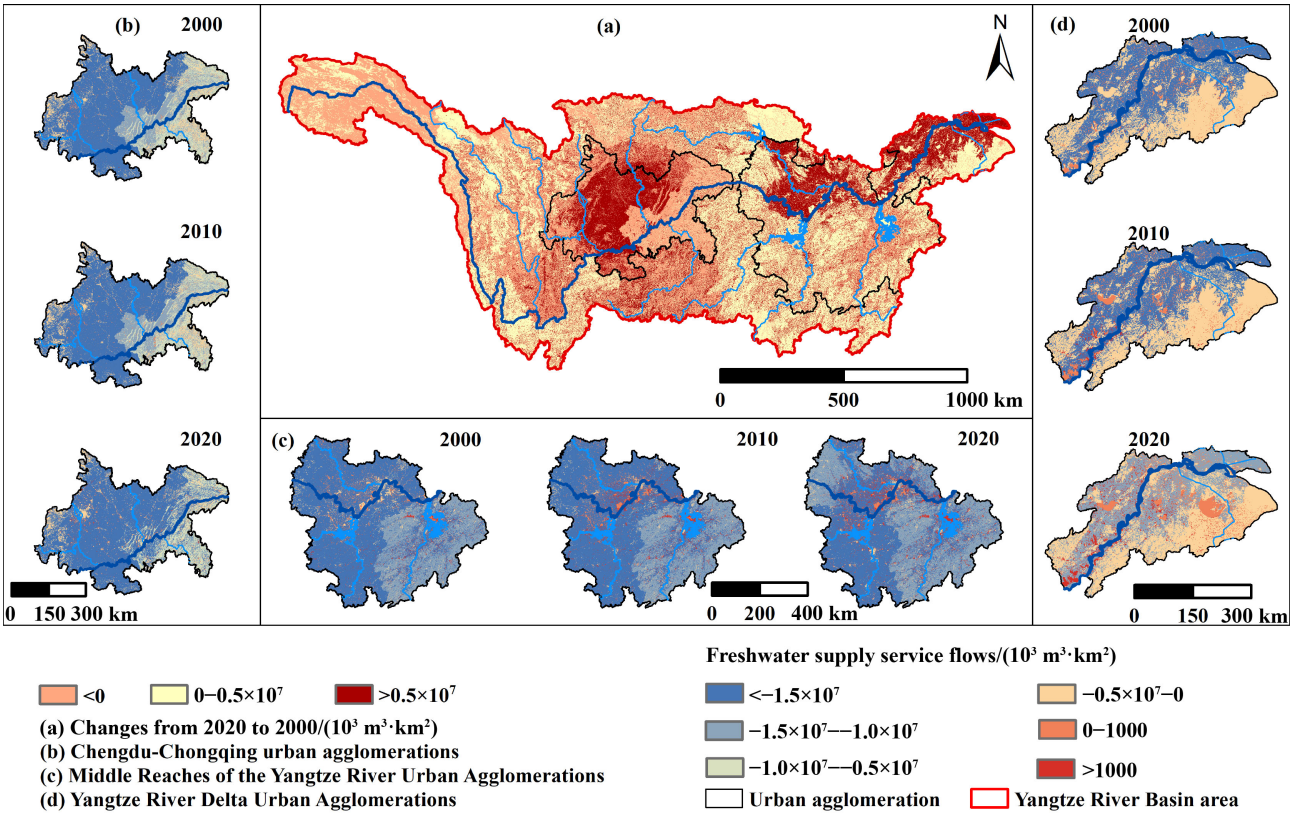

Fig. 12 The division of urban agglomerations of the YRB and freshwater supply service flows in different years.

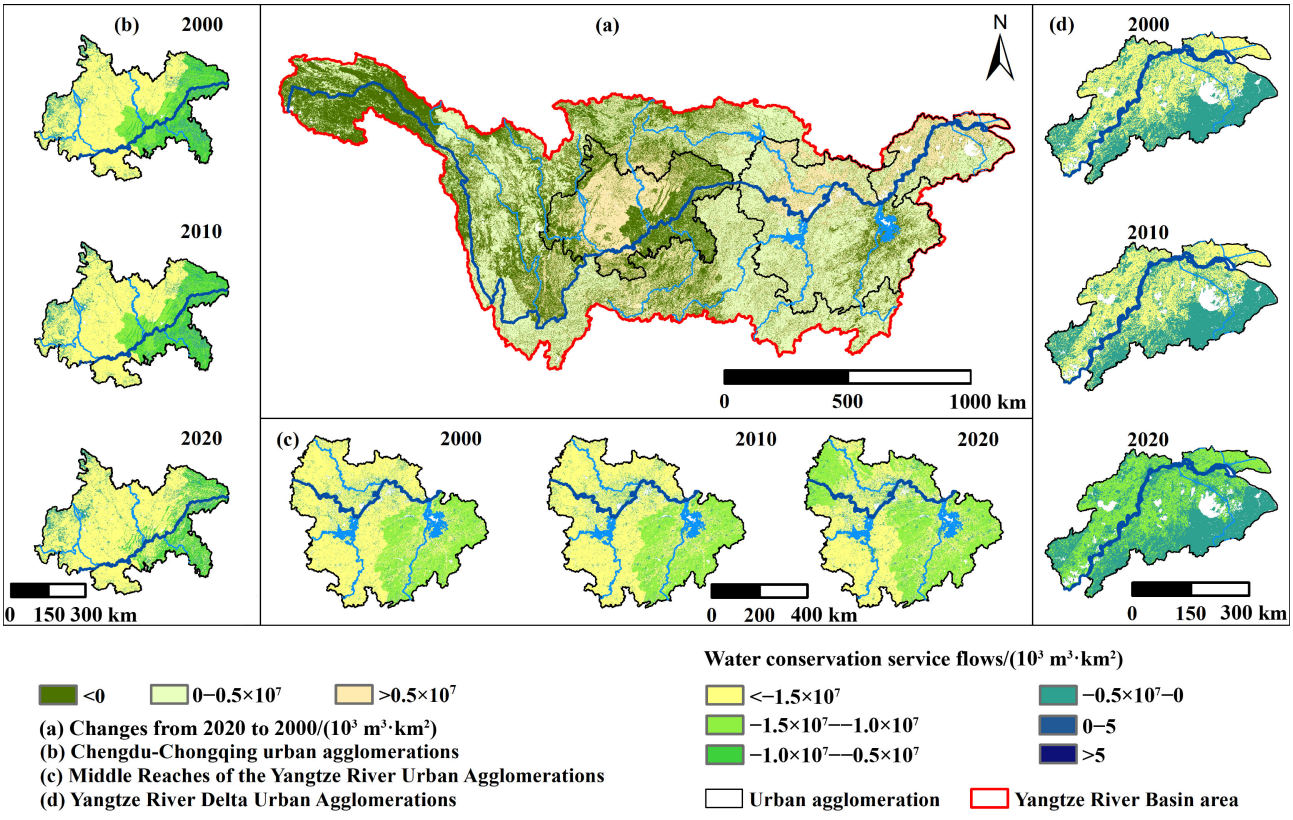

Fig. 13 The division of urban agglomerations of the YRB and water conservation service flows in different years.

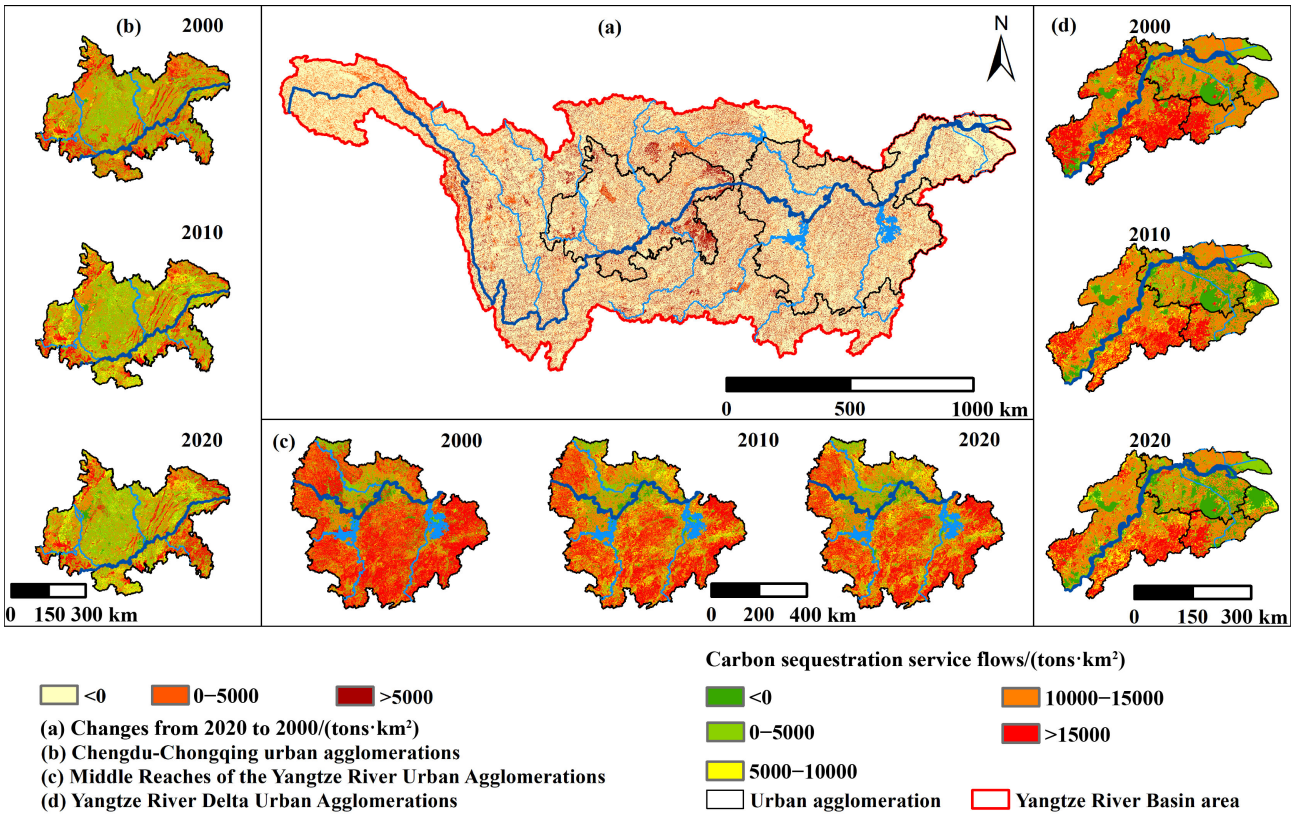

Fig. 14 The division of urban agglomerations of the YRB and carbon sequestration service flows in different years.

FSF capacity of the MRYRUA was low, while the *FSF* capacity of the YRDUA was high.

From 2000 to 2020, the water conservation service of the urban agglomeration in the YRB was in short supply, as shown in Fig. 13. The low-value region of the *FSF* in the CCUA steadily grew to the west (Fig. 13(b)), which is compatible with the geographical distribution of the *WCF*. In the MRYRUA, the high-value segment of the *WCF* progressively expanded to the north-west (Fig. 13(c)). From 2000 to 2010, the spatial differentiation of the *WCF* in the MRYRUA was not readily apparent, exhibiting a spatially distributed pattern with high values in the south-east and low values in the west. From 2010 to 2020, the spatial differentiation of the *WCF* in the MRYRUA was substantial, displaying a distributed spatial pattern with low values in the south-west. The low-value area of the *WCF* in the YRDUA gradually decreased to the south. From 2000 to 2010, the spatial dispersion of the *WCF* within the YRDUA remained relatively stable (Fig. 13(d)). From 2010 to 2020, the change in the *WCF* in the YRDUA was very significant. The YRDUA possessed a high capacity for *WCF*, and the CCUA had a minimal capacity.

From 2000 to 2020, the *CS* of the urban agglomerations in the YRB were generally in a state of oversupply, as shown in Fig. 14. The high-value region of the *CSF* in the CCUA decreased and then increased, exhibiting a spatially distributed pattern with low values in the center and high values on all sides (Fig. 14(b)). The spatial change in the *CSF* in the MRYRUA was not obvious, showing a spatial distribution pattern with low values in the north (Fig. 14(c)). The high-value area of the *CSF* in the YRDUA gradually increased, and a small part of the low-value area was discontinuous (Fig. 14(d)). The MRYRUA exhibited a high capacity for the flow of services related to carbon sequestration, and the YRDUA had a poor capacity for these services.

From 2000 to 2020, the *CRF* of the urban agglomerations in the YRB were generally in short supply, as shown in Fig. 15. The high-value region of the *CRF* in the CCUA decreased progressively to the east, exhibiting a spatially distributed pattern with low values in the center and high values on the edges (Fig. 15(b)). The low-value region of the *CRF* in the MRYRUA initially fell and then climbed northward, exhibiting a spatial dispersion pattern with high values in the north-west (Fig. 15(c)). The high-value area of the *CRF* in the YRDUA first increased and then decreased to the south-west and was scattered in a blocky pattern, showing a spatial dispersion pattern with low values in the south-west (Fig. 15(d)). The capacity of urban agglomerations in the YRB for the *CRF* was minimal.

The Yangtze River Economic Belt strategy is conducive to cultivating new impetus for developing urban agglomerations, but the constraints of resources and the environment are increasing. The construction land

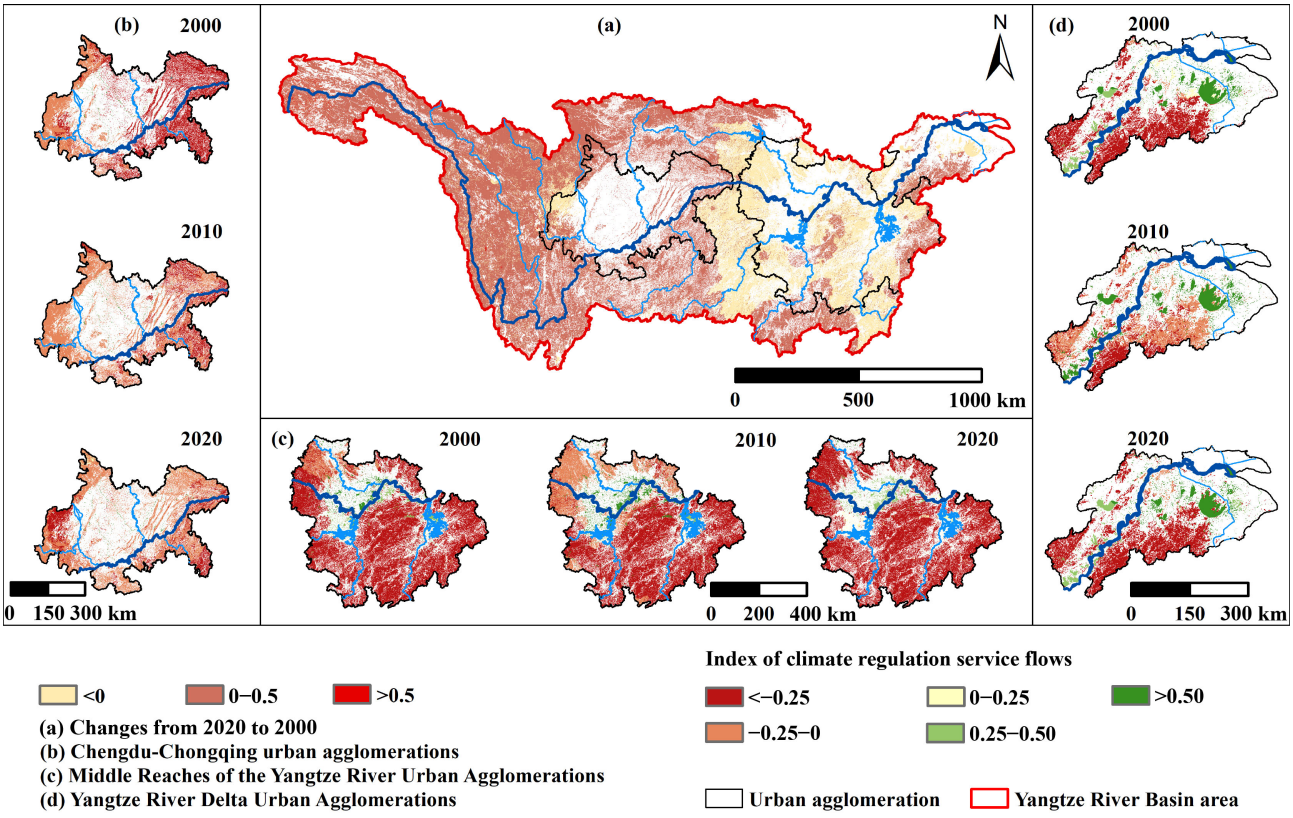

Fig. 15 The division of urban agglomerations of the YRB and climate regulation service flows in different years.

expansion in the CCUA has crowded out ecological land with a high ecosystem supply, such as forest land, grassland, and wetland. Environmental pollution and ecological bad events occur frequently (Luo et al., 2023). The demand for *FS* and *WC* has increased. The supply has weakened, and the *FSF* and *WCF* have gradually increased. In 2011, the "Chengdu-Chongqing Economic Regional Plan" was launched. With the optimisation of resource development and the construction of an ecological network framework, the ecological security guarantee area in the URYR was further constructed, and the capacity of *CS* and *CR* in the CCUA was gradually enhanced. In 2021, the "Outline of the Construction Plan for the Two-City Economic Circle in Chengdu-Chongqing Region" was issued to strengthen the protection of important ecological space further, improve the efficiency of land use, water use, and energy use, and focus on improving the stability and connectivity of the ecosystem to build an ecological protection zone in the URYR jointly.

In recent decades, the land use change of the MRYRUA has been severe, causing problems such as the loss of cultivated land and water resources, energy shortages, and landscape fragmentation (Liu et al., 2023b). The *FSF* and *WCF* gradually increased, and the *CSF* gradually decreased. Since the implementation of the "Development Plan of Urban Agglomeration in the Middle Reaches of the Yangtze River" in 2015, the contradiction between ecological protection and basic cultivated land protection is still very prominent (Hu et al., 2022). The MRYRUA is a key area of national food security. It is rich in precipitation and forest resources, and the *CRF* changes significantly. To promote the sustainable development of the MRYRUA, it is necessary to promote the green and low-carbon transformation further, strengthen the joint prevention and control of environmental pollution, and coordinate the implementation of ecological environment zoning control.

The YRDUA is riverside and coastal, the city spreads disorderly, the population pressure in the central urban area is large, the water quality of inland lakes deteriorates, and the wetland damage is serious (Gu et al., 2011; Tian and Mao, 2022). The ecosystem service flow of the whole urban agglomeration was low (Fig. 11). To improve the ecological quality of the YRDUA, the "Outline of the Yangtze River Delta Regional Integration Development Plan" was implemented in 2019. Building a high-standard farmland forest network, carrying out vegetation restoration, promoting water ecological restoration, and improving the cross-regional ecological compensation mechanism are necessary.

4.3 Zoning regulation path of the ecosystem service flows in the Yangtze River Basin

Through the supply and demand ratio model, CESDR in

the YRB in 2000, 2010, and 2020 was calculated. Depending on the aggregation state of the supply and demand matching relationship, the ecosystem service flows in the YRB were divided into a confluence area, flow area and outflow area (Guan et al., 2023; Shen et al., 2023; Tan et al., 2023a), as depicted in Fig. 16. The confluence area is an area with a serious mismatch between the supply and demand, and the supply-demand is low. The flow area is an area where the supply and demand are relatively matched. The supply and demand are ideal, and the supply service is relatively abundant. There is little shortage of supply. The supply service surplus may flow out to other areas, and the supply service surplus in other areas may also flow into the area. The supply services in the outflow area are relatively abundant, and the supply and demand are relatively high. The surplus of supply services can supplement the basins in other regions.

In 2000, the confluence areas mainly occurred in Sichuan, northern Guizhou, north-western Hubei and the junction of Hunan, Hubei and Jiangxi in the basin. The flow areas mainly occurred in Qinghai, Gansu and Shaanxi in the basin. The outflow areas were mainly located in Xizang, Yunnan, south-eastern Hubei, Jiangxi, Chongqing, and Hunan in the basin (Fig. 16(a)). The confluence area comprised 28.63% of the total region area, the flow area comprised 11.46%, and the outflow area comprised 59.91%. In 2010, the confluence areas were mainly predominantly in Qinghai and Sichuan. The flow areas primarily occurred in south-western Yunnan, Guizhou, eastern Gansu, and north-western Hunan. The outflow areas mainly occurred in Shaanxi, Chongqing, south-western Hunan, Hubei, Jiangxi, and south-eastern Anhui (Fig. 16(b)). The confluence area comprised 24.03% of the total area, the flow area comprised 8.62%, and the outflow area comprised 67.35% of the basin. In 2020, the confluence areas mainly occurred in Sichuan, Guizhou, northern Hunan, and south-eastern Hubei, the flow areas were mainly located in central Hubei, Guizhou, and north-western Jiangxi, and the outflow areas mainly occurred in Qinghai, Xizang, Shaanxi, Henan, Gansu, and south-eastern Anhui (Fig. 16(c)). Among these area types, the confluence area comprised 27.11% of the total basin area, the flow area comprised 3.61%, and the outflow area comprised 69.28%. From 2000 to 2020, the proportions of the confluence area exhibited a tendency of first falling and then rising, the flow area showed a trend of gradual decline, and the outflow area revealed a trend of gradual ascent.

Taking corresponding measures in different ecological zones is conducive to strengthening the protection and restoration of the regional ecological environment and promoting the sustainable development of regional science (Shen et al., 2023; Wu et al., 2023; Xia et al., 2023). For the confluence area of ES, strictly control the scale and intensity of construction land expansion, strengthen land law enforcement and supervision, and replenish cultivated land; we will adopt alternative technologies for fossil energy, improve the utilization rate of agricultural fertilizers, optimize the allocation of resources, and accelerate the green and low-carbon transformation. For the flow area of ES, it is urgent to promote the construction of a new socialist countryside and improve the living standards and quality of life of urban and rural residents; protect arable land and ensure national food security; appropriately increase the area of ecological land and improve the ecological supply capacity of the basin; we will appropriately accelerate the pace of urbanization, optimize the industrial structure, improve scientific and technological innovation facilities, and improve the overall development level of the region. For the outflow area of ES, solidly promote the protection forest along the Yangtze River Economic Belt, scientifically transform the ecological dividend into a development dividend, support the development of the eco-tourism industry, and improve the Yangtze River Protection Law.

5 Conclusions

This study quantified the supply, demand and flow of four kinds of ES in the YRB from 2000 to 2020 at three spatial scales: watershed, urban agglomeration and province. It proposed the regionalization control path for ecosystem service flow in the study area. From 2000 to

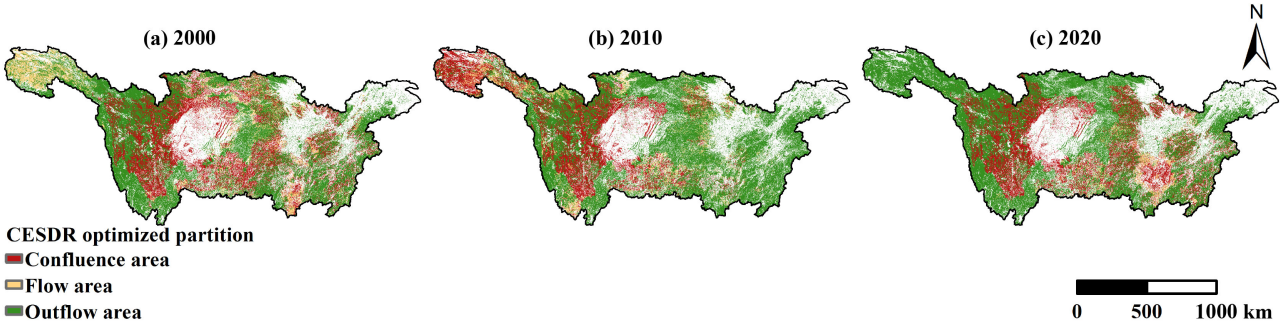

Fig. 16 Optimization zoning of comprehensive supply and demand ratio of ecosystem services in the YRB in 2000, 2010 and 2020.

2020, there was a general decreasing trend in the *FSF*, the *WCF*, and the *CSF*, with corresponding fall rates of 10.90%, 11.11%, and 5.17%. With a drop rate of 35.53%, the *CRF* displayed a pattern of initially falling and rising activity. In terms of distribution spatially, the *FS*, *CS*, and *CR* were in short supply in the densely populated areas of the YRB, while the other areas exhibited an excess of demand; water conservation in the north-west of the area was oversupplied, while that in the south-east was in short supply. At the provincial scale, the service flows of *FS*, *WC*, and *CS* in Sichuan Province were the highest, the service flows of *FS* and *WC* in Fujian and Xizang were low, the service flow of *CS* in Guangdong Province was the lowest, the annual average *CRF* in Jiangxi Province was the highest, and the *CRF* in Qinghai Province was the lowest. The lowest was the ecosystem service flow in the LRYR and the YRDUA. The *FSF* and *WCF* were the highest in the URYR and the CCUA. The *CSF* and *CRF* were the highest in the MRYR and the MRYRUA. In 2000, Sichuan, northern Guizhou, and north-western Hubei in the YRB were confluence areas; Qinghai, eastern Shaanxi, and south-western Hubei were flow areas; and Yunnan, Xizang, south-eastern Hubei, and Jiangxi were outflow areas. In 2010, Sichuan and Qinghai in the YRB were confluence areas, Guizhou and north-west Hubei were flow areas, and Hubei, Jiangxi, Yunnan, and Chongqing were outflow areas. In 2020, Sichuan and eastern Hubei in the YRB were confluence areas; Guizhou and north-western Hubei were flow areas; and Qinghai, Xizang, Chongqing, Gansu, Shaanxi, and south-eastern Anhui were outflow areas. From 2000 to 2020, the change ratios of the area proportion of the confluence, flow, and outflow areas in the YRB were 1.06, 3.17, and 0.86, respectively. The research results had high scientific significance and positive practical significance for regulating ES and promoting regional sustainable development in the YRB.

Data availability The data sets generated during and/or analyzed during the current study are available from the corresponding author on reasonable request.

Competing interest The authors declare that they have no competing interests.

Acknowledgments This work was supported by the National Natural Science Foundation of China (Grant Nos. 42171298 and 42201333), Late Project of the National Social Science Foundation in China (No. 20FJYB035) and Natural Science Foundation of Chongqing, China (No. cstc2020jcyj-jqX0004).

References

Abdelrhman H A, Almaleeh T A, Elshareef I M M (2022). Economic valuation of ecosystem services provided by Dellanj Forest using contingent valuation methods. J Economics Public Finance, 8(4): 58

Assis J C, Hohlenwerger C, Metzger J P, Rhodes J R, Duarte G T, Da Silva R A, Boesing A L, Prist P R, Ribeiro M C (2023). Linking landscape structure and ecosystem service flow. Ecosyst Serv, 62: 101535

Brooks E B, Coulston J W, Riitters K H, Wear D N (2020). Using a hybrid demand-allocation algorithm to enable distributional analysis of land use change patterns. PLoS One, 15(10): e0240097

Cao L, Kong F, Xu C (2022). Exploring ecosystem carbon storage change and scenario simulation in the Qiantang River source region of China. Sci Prog, 105(3): 1–26

Chen D, Li J, Yang X, Zhou Z, Pan Y, Li M (2020). Quantifying water provision service supply, demand and spatial flow for land use optimization: a case study in the Yanhe watershed. Ecosyst Serv, 43: 101117

Dang K B, Burkhard B, Dang V B, Vu K C (2020). Potential, flow and demand of rice provisioning ecosystem services – case study in Sapa district, Vietnam. Ecol Indic, 118: 106731

Deng C, Zhu D, Liu Y, Li Z (2022). Spatial matching and flow in supply and demand of water provision services: a case study in Xiangjiang River Basin. J Mt Sci, 19(1): 228–240

Du H, Zhao L, Zhang P, Li J, Yu S (2023). Ecological compensation in the Beijing-Tianjin-Hebei region based on ecosystem services flow. J Environ Manage, 331: 117230

Duan H, Xu N (2022). Assessing social values for ecosystem services in rural areas based on the SolVES Model: a case study from Nanjing, China. Forests, 13(11): 1877

Fang L, Wang L, Chen W, Sun J, Cao Q, Wang S, Wang L (2021). Identifying the impacts of natural and human factors on ecosystem service in the Yangtze and Yellow River Basins. J Clean Prod, 314: 127995

Feurer M, Rueff H, Celio E, Heinimann A, Blaser J, Htun A M, Zaehringer J G (2021). Regional scale mapping of ecosystem services supply, demand, flow and mismatches in Southern Myanmar. Ecosyst Serv, 52: 101363

Fisher B, Turner R K, Morling P (2009). Defining and classifying ecosystem services for decision making. Ecol Econ, 68(3): 643–653

Gao Y, Wang Z, Xu F (2023). Geospatial characteristics and the application of land use functions in the Yangtze River Economic Belt, China: perspectives on provinces and urban agglomerations. Ecol Indic, 155: 110969

Geng W, Li Y, Zhang P, Yang D, Jing W, Rong T (2022). Analyzing spatio-temporal changes and trade-offs/synergies among ecosystem services in the Yellow River Basin, China. Ecol Indic, 138: 108825

Granado-Díaz R, Gómez-Limón J A, Rodríguez-Entrena M, Villanueva A J (2020). Spatial analysis of demand forsparsely located ecosystem services using alternative index approaches. Eur Rev Agric Econ, 47: 752–784

Gu C, Hu L, Zhang X, Wang X, Guo J (2011). Climate change and urbanization in the Yangtze River Delta. Habitat Int, 35(4): 544–552

Guan D, Deng Z, Zhou L L, Fan X, Yang W, Peng G, Zhu X, Zhou L J (2023). How can multiscenario flow paths of water supply services be simulated? A supply-flow-demand model of ecosystem services across a typical basin, in China. Sci Total Environ, 893: 164770

Guan D, Wu L, Cheng L, Zhang Y, Zhou L (2022). How to measure the ecological compensation threshold in the upper Yangtze River basin, China? An approach for coupling InVEST and grey water

footprint. Front Earth Sci (Lausanne), 10: 988291

Hochmalová M, Purwestri R C, Jian Y, Jarský V, Riedl M, Dian Y, Hájek M (2022). Demand for forest ecosystem services: a comparison study in selected areas in the Czech Republic and China. Eur J For Res, 141(5): 867–886

Hu N, Xu D, Zou N, Fan S, Wang P, Li Y (2023). Multi-scenario simulations of land use and habitat quality based on a PLUS-InVEST Model: a case study of Baoding, China. Sustainability (Basel), 15(1): 557

Hu Y, Liu Y, Li C (2022). Multi-scenario simulation of land use change and ecosystem service value in the middle reaches of Yangtze River urban agglomeration. Sustainability, 14(23): 15738

Huang M, Xiao Y, Xu J, Liu J, Wang Y, Gan S, Lv S, Xie G (2022). A review on the supply-demand relationship and spatial flows of ecosystem services. J Resour Ecol, 13: 925–935

Jia Q, Jiao L, Lian X, Wang W (2023). Linking supply-demand balance of ecosystem services to identify ecological security patterns in urban agglomerations. Sustain Cities Soc, 92: 104497

Jiang W, Fu B, Gao G, Lv Y, Wang C, Sun S, Wang K, Schüler S, Shu Z (2023). Exploring spatial-temporal driving factors for changes in multiple ecosystem services and their relationships in West Liao River Basin, China. Sci Total Environ, 904: 166716

Jiang Y, Guan D, He X, Yin B, Zhou L, Sun L, Huang D, Li Z, Zhang Y (2022). Quantification of the coupling relationship between ecological compensation and ecosystem services in the Yangtze River Economic Belt, China. Land Use Policy, 114: 105995

Li Z, Guan D, Zhou L, Zhang Y (2022). Constraint relationship of ecosystem services in the Yangtze River Economic Belt, China. Environ Sci Pollut Res Int, 29(9): 12484–12505

Lin J, Huang J, Prell C, Bryan B A (2021). Changes in supply and demand mediate the effects of land-use change on freshwater ecosystem services flows. Sci Total Environ, 763: 143012

Lin Y, Zhang M, Gan M, Huang L, Zhu C, Zheng Q, You S, Ye Z, Shahtahmassebi A R, Li Y, Deng J, Zhang J, Zhang L, Wang K (2022). Fine identification of the supply–demand mismatches and matches of urban green space ecosystem services with a spatial filtering tool. J Clean Prod, 336: 130404

Liu H, Xiao W, Zhu J, Zeng L, Li Q (2022a). Urbanization intensifies the mismatch between the supply and demand of regional ecosystem services: a large-scale case of the Yangtze River economic belt in China. Remote Sens (Basel), 14(20): 5147

Liu J, Chen X, Chen W, Zhang Y, Wang A, Zheng Y (2023a). Ecosystem service value evaluation of saline—alkali land development in the Yellow River Delta—the example of the Huanghe Island. Water, 15(3): 477

Liu M, Xiong Y, Zhang A (2023b). Multi-scale telecoupling effects of land use change on ecosystem services in urban agglomerations –A case study in the middle reaches of Yangtze River urban agglomerations. J Clean Prod, 415: 137878

Liu Q, Sun X, Wu W, Liu Z, Fang G, Yang P (2022b). Agroecosystem services: a review of concepts, indicators, assessment methods and future research perspectives. Ecol Indic, 142: 109218

Liu Z, Rong L, Wei W (2023c). Impacts of land use/cover change on water balance by using the SWAT model in a typical loess hilly watershed of China. Geogr Sustain, 4(1): 19–28

Luo T, Zeng J, Chen W, Wang Y, Gu T, Huang C (2023). Ecosystem services balance and its influencing factors detection in China: a case study in Chengdu-Chongqing urban agglomerations. Ecol Indic, 151: 110330

Lyu Y, Wu C (2023). Managing the supply-demand mismatches and potential flows of ecosystem services from the perspective of regional integration: a case study of Hangzhou, China. Sci Total Environ, 902: 165918

Ma Z, Gong J, Hu C, Lei J (2023). An integrated approach to assess spatial and temporal changes in the contribution of the ecosystem to sustainable development goals over 20 years in China. Sci Total Environ, 903: 166237

Meng Q, Zhang L, Wei H, Cai E, Xue D, Liu M (2021). Linking ecosystem service supply–demand risks and regional spatial management in the Yihe River Basin, Central China. Land (Basel), 10(8): 843

Müller F, Bicking S, Ahrendt K, Kinh Bac D, Blindow I, Fürst C, Haase P, Kruse M, Kruse T, Ma L, Perennes M, Ruljevic I, Schernewski G, Schimming C G, Schneiders A, Schubert H, Schumacher J, Tappeiner U, Wangai P, Windhorst W, Zeleny J (2020). Assessing ecosystem service potentials to evaluate terrestrial, coastal and marine ecosystem types in Northern Germany – an expert-based matrix approach. Ecol Indic, 112: 106116

Palomo I, Martín-López B, Potschin M, Haines-Young R, Montes C (2013). National Parks, buffer zones and surrounding lands: mapping ecosystem service flows. Ecosyst Serv, 4: 104–116

Pan Z, Gao G, Fu B (2022). Spatiotemporal changes and driving forces of ecosystem vulnerability in the Yangtze River Basin, China: quantification using habitat-structure-function framework. Sci Total Environ, 835: 155494

Peng L, Zhang L, Li X, Wang P, Zhao W, Wang Z, Jiao L, Wang H (2022). Spatio-temporal patterns of ecosystem services provided by urban green spaces and their equity along urban–rural gradients in the Xi'an Metropolitan Area, China. Remote Sens (Basel), 14(17): 4299

Qin K, Liu J, Yan L, Huang H (2019). Integrating ecosystem services flows into water security simulations in water scarce areas: present and future. Sci Total Environ, 670: 1037–1048

Sauter I, Kienast F, Bolliger J, Winter B, Pazúr R (2019). Changes in demand and supply of ecosystem services under scenarios of future land use in Vorarlberg, Austria. J Mt Sci, 16(12): 2793–2809

Schirpke U, Egarter Vigl L, Tasser E, Tappeiner U (2019). Analyzing spatial congruencies and mismatches between supply, demand and flow of ecosystem services and sustainable development. Sustainability (Basel), 11(8): 2227

Schuwirth N, Borgwardt F, Domisch S, Friedrichs M, Kattwinkel M, Kneis D, Kuemmerlen M, Langhans S D, Martínez-López J, Vermeiren P (2019). How to make ecological models useful for environmental management. Ecol Modell, 411: 108784

Serna-Chavez H M, Schulp C, Van Bodegom P M, Bouten W, Verburg P H, Davidson M D (2014). A quantitative framework for assessing spatial flows of ecosystem services. Ecol Indic, 39: 24–33

Shaad K, Souter N J, Vollmer D, Regan H M, Bezerra M O (2022). Integrating ecosystem services into water resource management: an

indicator-based approach. Environ Manage, 69(4): 752–767

Shen J, Li S C, Wang H, Wu S, Liang Z, Zhang Y T, Wei F, Li S, Ma L, Wang Y, Liu L, Zhang Y J (2023). Understanding the spatial relationships and drivers of ecosystem service supply-demand mismatches towards spatially-targeted management of social-ecological system. J Clean Prod, 406: 136882

Sheng J, Rui D, Han X (2022). Governmentality and sociotechnical imaginary within the conservation-development nexus: China's Great Yangtze River Protection Programme. Environ Sci Policy, 136: 56–66

Shi Y, Shi D, Zhou L, Fang R (2020). Identification of ecosystem services supply and demand areas and simulation of ecosystem service flows in Shanghai. Ecol Indic, 115: 106418

Song J, Liang Z, Guo Q, Wang C (2023). Current situation, dilemmas and measures to improve horizontal ecological compensation coordination mechanisms in river basins. Sustainability (Basel), 15(2): 1504

Stürck J, Poortinga A, Verburg P H (2014). Mapping ecosystem services: the supply and demand of flood regulation services in Europe. Ecol Indic, 38: 198–211

Tan J, Peng L, Wu W, Huang Q (2023a). Mapping the evolution patterns of urbanization, ecosystem service supply–demand, and human well-being: a tree-like landscape perspective. Ecol Indic, 154: 110591

Tan L, Yang G, Zhu Q, Wan R, Shi K (2023b). Optimizing payment for ecosystem services in a drinking water source watershed by quantifying the supply and demand of soil retention service. J Environ Manage, 331: 117303

Tao Y, Tao Q, Sun X, Qiu J, Pueppke S G, Ou W, Guo J, Qi J (2022). Mapping ecosystem service supply and demand dynamics under rapid urban expansion: a case study in the Yangtze River Delta of China. Ecosyst Serv, 56: 101448

Tian Y, Mao Q (2022). The effect of regional integration on urban sprawl in urban agglomeration areas: a case study of the Yangtze River Delta, China. Habitat Int, 130: 102695

Tindale S, Vicario-Modroño V, Gallardo-Cobos R, Hunter E, Miškolci S, Price P N, Sánchez-Zamora P, Sonnevelt M, Ojo M, McInnes K, Frewer L (2023). Citizen perceptions and values associated with ecosystem services from European grassland landscapes. Land Use Policy, 127: 106574

Vergarechea M, Astrup R, Fischer C, Øistad K, Blattert C, Hartikainen M, Eyvindson K, Di Fulvio F, Forsell N, Burgas D, Toraño-Caicoya A, Mönkkönen M, Antón-Fernández C (2023). Future wood demands and ecosystem services trade-offs: a policy analysis in Norway. For Policy Econ, 147: 102899

Wang C, Zhao M, Xu Y, Zhao Y, Zhang X (2023). Ecosystem service synergies promote ecological tea gardens: a case study in Fuzhou, China. Remote Sens (Basel), 15(2): 540

Wang H, Wang L, Fu X, Yang Q, Wu G, Guo M, Zhang S, Wu D, Zhu Y, Deng H (2022a). Spatial-temporal pattern of ecosystem service supply-demand and coordination in the Ulansuhai Basin, China. Ecol Indic, 143: 109406

Wang L, Zheng H, Chen Y, Ouyang Z, Hu X (2022b). Systematic review of ecosystem services flow measurement: main concepts, methods, applications and future directions. Ecosyst Serv, 58: 101479

Wang R, Zhang Y, Zhang H, Yu H (2022c). Social value assessment and spatial expression of national park ecosystems based on residents' perceptions. Sustainability (Basel), 14(7): 4206

Wu J, Fan X, Li K, Wu Y (2023). Assessment of ecosystem service flow and optimization of spatial pattern of supply and demand matching in Pearl River Delta, China. Ecol Indic, 153: 110452

Wu J, Huang Y, Jiang W (2022). Spatial matching and value transfer assessment of ecosystem services supply and demand in urban agglomerations: a case study of the Guangdong-Hong Kong-Macao Greater Bay area in China. J Clean Prod, 375: 134081

Wu W, Tang H, Yang P, You L, Zhou Q, Chen Z, Shibasaki R (2011). Scenario-based assessment of future food security. J Geogr Sci, 21(1): 3–17

Xia H, Yuan S, Prishchepov A V (2023). Spatial-temporal heterogeneity of ecosystem service interactions and their social-ecological drivers: implications for spatial planning and management. Resour Conserv Recycling, 189: 106767

Xia P, Chen B, Gong B, Liu Z, He C, Wang Y (2022). The supply and demand of water purification service in an urbanizing basin on the Tibetan Plateau. Landsc Ecol, 37(7): 1937–1955

Xiang H, Zhang J, Mao D, Wang Z, Qiu Z, Yan H (2022). Identifying spatial similarities and mismatches between supply and demand of ecosystem services for sustainable northeast China. Ecol Indic, 134: 108501

Xu D, Zhang Y (2022). Identifying the flow paths and beneficiary ranges of the sand fixation service: a case-study in Xilingol League, China. Land Degrad Dev, 33(3): 413–424

Xu Z, Peng J (2022). Ecosystem services-based decision-making: a bridge from science to practice. Environ Sci Policy, 135: 6–15

Xue C, Chen X, Xue L, Zhang H, Chen J, Li D (2023). Modeling the spatially heterogeneous relationships between tradeoffs and synergies among ecosystem services and potential drivers considering geographic scale in Bairin Left Banner, China. Sci Total Environ, 855: 158834

Xue D, Wang Z, Li Y, Liu M, Wei H (2022). Assessment of ecosystem services supply and demand (Mis)matches for urban ecological management: a case study in the Zhengzhou–Kaifeng–Luoyang cities. Remote Sens (Basel), 14(7): 1703

Yan X, Li L (2023). Spatiotemporal characteristics and influencing factors of ecosystem services in Central Asia. J Arid Land, 15(1): 1–19

Yan X, Liu C, Han Z, Li X, Zhong J (2023). Spatiotemporal assessment of ecosystem services supply–demand relationships to identify ecological management zoning in coastal city Dalian, China. Environ Sci Pollut Res Int, 30(23): 63464–63478

Yang H, Zhong X, Deng S, Nie S (2022a). Impact of LUCC on landscape pattern in the Yangtze River Basin during 2001–2019. Ecol Inform, 69: 101631

Yang M, Zhao X, Wu P, Hu P, Gao X (2022b). Quantification and spatially explicit driving forces of the incoordination between ecosystem service supply and social demand at a regional scale. Ecol Indic, 137: 108764

Yin D, Yu H, Shi Y, Zhao M, Zhang J, Li X (2023). Matching supply and demand for ecosystem services in the Yellow River Basin,

China: a perspective of the water-energy-food nexus. J Clean Prod, 384: 135469

Yu H, Xie W, Sun L, Wang Y (2021). Identifying the regional disparities of ecosystem services from a supply-demand perspective. Resour Conserv Recycling, 169: 105557

Yuan Y, Bai Z, Zhang J, Huang Y (2023). Investigating the trade-offs between the supply and demand for ecosystem services for regional spatial management. J Environ Manage, 325: 116591

Zhang J, He C, Huang Q, Li J, Qi T (2022a). Evaluating the supply and demand of cultural ecosystem services in the Tibetan Plateau of China. Landsc Ecol, 37(8): 2131–2148

Zhang L, Li J (2022). Identifying priority areas for biodiversity conservation based on Marxan and InVEST model. Landsc Ecol, 37(12): 3043–3058

Zhang S, Wang Y, Wang Y, Li Z, Hou Y (2023). Spatiotemporal evolution and influencing mechanisms of ecosystem service value in the Tarim River Basin, northwest China. Remote Sens (Basel), 15(3): 591

Zhang X, Chen P, Dai S, Han Y (2022b). Assessment of the value of regional water conservation services based on SWAT model. Environ Monit Assess, 194(8): 559

Zhang X, Zhang G, Long X, Zhang Q, Liu D, Wu H, Li S (2021). Identifying the drivers of water yield ecosystem service: a case study in the Yangtze River Basin, China. Ecol Indic, 132: 108304

Zhao Y, Wang N, Luo Y, He H, Wu L, Wang H, Wang Q, Wu J (2022). Quantification of ecosystem services supply-demand and the impact of demographic change on cultural services in Shenzhen, China. J Environ Manage, 304: 114280

Zheng L, Liu H, Huang Y, Yin S, Jin G (2020). Assessment and analysis of ecosystem services value along the Yangtze River under the background of the Yangtze River protection strategy. J Geogr Sci, 30(4): 553–568

Zhou L, Guan D, Yuan X, Zhang M, Gao W (2021). Quantifying the spatiotemporal characteristics of ecosystem services and livelihoods in China's poverty-stricken counties. Front Earth Sci, 15(3): 553–579

Zhou L, Zhang H, Bi G, Su K, Wang L, Chen H, Yang Q (2022). Multiscale perspective research on the evolution characteristics of the ecosystem services supply-demand relationship in the Chongqing section of the three gorges reservoir area. Ecol Indic, 142: 109227

Zhu Y (2022). Social value evaluation of ecosystem services in global geoparks based on SolVES model. Math Probl Eng, 2022: 9748880

Zou W, He Y, Ye B, Zhao X, Xu D, Xiao R, Duan Y (2021). Study on carbon storage of ecosystem in Qianjiangyuan national park based on InVEST model. J Cent South Univ, 41: 120–128

Zou Z Y, Xiao Y, Ouyang Z Y, Song C S, Wang K L (2019). Evaluation of the effectiveness of ecological protection in Qiandongnan Miao-Dong Autonomous Prefecture. Acta Ecol Sin, 39(4): 1407–1415